YTUP

Journal of Thermal Engineering
https://jten.yildiz.edu.tr/
https://doi.org/10.47481/jten.0012

REVIEW ARTICLE

Performance improvements of solar evacuated tube collectors: a literature review

Manishkumar D. Mathukia[1*] Dr. Karan H. Motwani[2] Dr. Nikhil J. Chotai[3,*]

[1]Research Scholar, Marwadi University, Rajkot, Gujarat, 360003, India and Lecturer in Mechanical Engineering, Government Polytechnic, Junagadh, Gujarat, 362263, India
[2]Mechanical Engineering Department, Faculty of Engineering & Technology, Marwadi University, Rajkot, Gujarat, 360003, India
[3]Mechanical Engineering Department, Faculty of Engineering & Technology, Marwadi University, Rajkot, Gujarat, 360003, India

Abstract

Evacuated-tube solar collectors have been shown to be effective medium-temperature solar thermal collectors, with improved insulation and less heat loss than flat-plate collectors. To enhance their usage and performance, various enhancement techniques have been explored. This review comprehensively integrates experimental and numerical studies of the five most frequently mentioned enhancement techniques: nanofluids, phase-change materials, reflectors/concentrators, design modifications and hybrid methods. Comparative evaluation reveals average efficiency improvements of 38.19% for hybrid, 28.03% for design modifications, 24.29% for phase change materials, 22.84% for nanofluids, and 20.40% for reflector/concentrators. The efficiency ranges reported in the studies vary widely, due to the strong influence of collector geometry, material characteristics and testing procedures. Optical misalignment and shading losses of the concentrator, dispersion stability and nanofluid abrasion, and cycling durability and leakage in the case of phase change materials are key issues. Along with reviewing the performance data, this study highlights key inconsistencies in the definition of baselines, test protocols and reporting approaches that affect the inter-study comparability. The novelty of the review is the aggregated efficiency gains reported for each category, the reporting of bias and the research agenda, which emphasises addressing the limitations of standardised testing, durability over time, and techno-economic and life-cycle considerations. Closing such gaps is crucial to make evacuated tube collectors trendsetting at the laboratory scale, and therefore affordable, effective and scalable for renewable energy applications.

Keywords: Evacuated tube collector, nanofluid, phase change material, reflector/concentrator, design modification, hybrid method

Cite this article as: Mathukia, M. D., Motwani, K. H., & Chotai, N. J. (2026). Performance improvements of solar evacuated tube collectors: A literature review. Journal of Thermal Engineering, 12(3), 1009–1045. https://doi.org/10.47481/jten.0012

1. Introduction

The world's energy demands and environmental challenges have created a demand for alternative energy sources; in particular, solar energy. The potential of solar energy as an alternative, cheaper, renewable energy source is vast, and can be used to reduce the use of fossil fuels and greenhouse gas emissions [1, 2]. At COP28, countries committed to increasing the world's renewable energy capacity at least threefold to 11.17 TW by 2030, making it clear that the implementation process requires bold and concerted action plans [3]. India, in turn, has also committed to a 500 GW solar target by 2030, supported by policies to address the challenge areas of storage, grid integration, and finance [4]. The numerous technologies involved in utilising solar energy, such as solar thermal collectors, are the ones that have been held responsible for transforming solar radiation into beneficial heat that can be used for water heating, space heating, industrial process heating, and solar cooling [5].

The two primary categories of solar thermal collectors are non-concentrating and concentrating. The non-concentrating flat-plate collectors (FPCs) have been the most popular choice in the past, owing to their low-cost configuration and design; they are best suited for applications where lower temperatures are employed (30-80°C). Concentrating collectors, on the other

*Corresponding Author
E-mail Adress: manishkumar.mathukia131181@marwadiuniversity.ac.in

Submitted: 10 October 2025; **Accepted:** 18 October 2025

This paper was recommended for publication in revised form by Editorin-Chief Ahmet Selim Dalkılıç

hand, are most suitable for high-temperature heat generation (above 300°C) for power generation, but are limited by their expense and complex design [6]. The non-concentrating type evacuated tube collectors (ETCs), as shown in Figure 1, have become a promising option, falling between FPCs and concentrating collectors, with higher efficiency than FPCs, particularly at low-to-medium temperatures [7], and better cost-effectiveness than concentrating collectors.

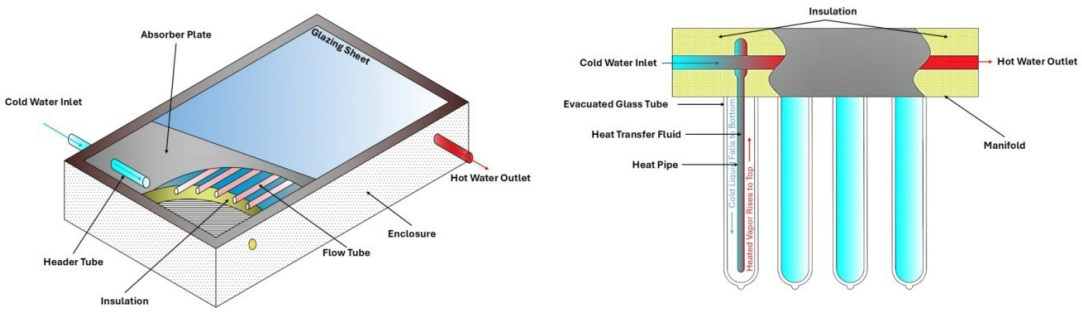

Figure 1. Schematic of flat plate (left) & evacuated tube (right) collectors

ETCs also offer advantages over other collector types, including superior thermal performance, lower heat loss, and the ability to operate under diffuse sunlight conditions. The evacuated space between the glass tubes reduces convective and conductive heat losses, thereby providing higher operating temperatures and improved overall efficiency. This makes ETCs viable in a wide range of applications, including the production of domestic hot water, solar-assisted heating and cooling systems, and industrial process heat. Their recent popularity in residential markets in China, Europe, and Japan reflects their increased adoption. This is due to the fact that there has been an increase in the availability of ETC and, consequently, a drop in prices [8]. With the increasing need for ETCs in solar thermal energy, there is a need to enhance their efficiency and increase their usefulness through performance enhancement. Several approaches have been taken to enhance the efficiency of ETCs [9]. These include, but are not limited to, the utilization of nanofluids, integration of PCM, incorporation of reflectors/concentrators, implementation of design alterations, hybrid methods, and the application of advanced control strategies. Figure 2 presents data from an open search of the Scopus database, illustrating the number of publications on solar ETCs from 2000 to 2024. The publications were identified using the keywords "solar AND evacuated AND tube AND collector." The graph shows a long-term growth in research interest, with the number of publications initially low in the early 2000s, increasing over time in the late 2000s and early 2010s, then increasing more significantly after 2014. The greatest increase occurred in the late 2010s and early 2020s, with a peak in 2021-2022. There has been an increased focus on evacuated-tube technologies and research on them in recent years.

Review and research papers have been written on methods of improving the performance of ETCs, such as nanofluids, PCMs, reflectors, concentrators, geometric profiling and hybrid approaches. All authors concurred that measurable gains can be made, but they also acknowledged that the test conditions and procedures employed can have a considerable impact on the outcomes. Hybrid techniques are most likely to provide the greatest improvements, but also introduce complexity. This paper adds to the existing body of knowledge by performing a systematic and comprehensive literature review, offering a quantitative analysis of average efficiency improvements, identifying biases in the literature and further clarifying the application of ETCs. This review seeks to provide an overview of methods to improve the thermal performance of ETCs and to determine the most effective approaches to enhance the thermal efficiency of ETCs while taking into account efficiency, cost and feasibility. The review also discusses the limitations and opportunities for future research on ETCs, offering guidance to researchers and practitioners.

This paper is divided into the following sections and subsections: introduction to evacuated-tube collectors; methods for enhancing thermal performance (use of nanofluids; use of phase-change materials; use of reflectors/concentrators; use of design modifications; hybrid strategies; comparative analysis); societal value; conclusion; and future work.

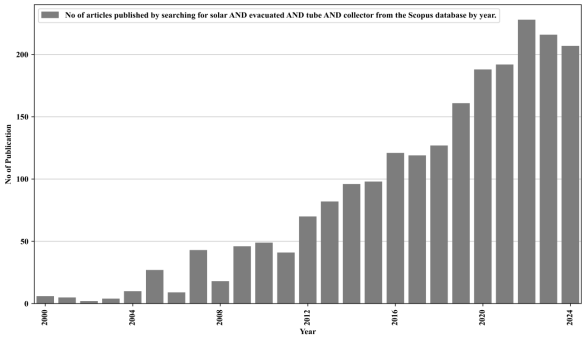

Figure 2. Number of Scopus-indexed articles per year on solar evacuated tube collectors (2000-2024)

2. Background of evacuated tube collectors

ETCs have been used as an alternative to FPCs, primarily because of their ability to effectively minimise heat loss, which is one of the key factors affecting the overall collector efficiency [10]. The underlying technology of ETCs is based on creating a vacuum between the absorber and the outer glass tube, which eliminates heat losses due to conduction and convection [11]. This feature allows ETCs to perform better, especially at higher temperatures, making them suitable for a variety of applications, such as domestic hot-water and process heat. The main elements of an ETC typically consist of the evacuated tube, an absorber fin or plate (often coated with a selective coating to promote solar absorption and reduce thermal emittance), a heat transfer medium (HTM, which can be a liquid, e.g., water or antifreeze solution, or a heat pipe containing a working fluid), and an insulated manifold that collects the hot fluid. The absorber absorbs the solar radiation and converts it to heat. The heat is efficiently transferred to the heat pipe or HTF and then transported to the manifold for use or storage. ETCs are relatively insensitive to the angle of incidence of the sun, and thus offer superior performance to FPCs under diffuse radiation [12]. The vacuum in the tube enclosure not only minimises heat loss but also extends the lifespan of the collector, thus delivering consistent performance for many years. ETCs are also favourable from a practical point of view as they do not need to be tracked by the sun and can operate over a wide range of temperatures.

ETCs can be categorised according to their design and operating principles. The primary types are direct-flow ETC and heat-pipe ETC [13], as shown in Figure 3. In direct-flow ETC, the HTF is circulated directly through the absorber tube and heat is transferred to the HTF as the fluid flows through the collector. In heat-pipe ETCs, a heat pipe is used to efficiently transfer heat from the vacuum tube to the manifold. The heat pipe is filled with a phase-change working fluid, which vaporises in the absorber, rises to the manifold condenser, condenses and returns to the absorber in a closed loop. In addition to these broad classifications, ETCs can also be sub-classified by absorber coating, absorber shape and evacuated tube shape (single-ended or double-ended). Further, the ETC design must take into account environmental considerations. For instance, in very cold climates, ETC designs must address freezing issues, by using antifreeze, or freeze-protection devices. Hot climates may cause overheating; this can be prevented by increasing the heat transfer area or by using high, selective thermal emissivity coating.

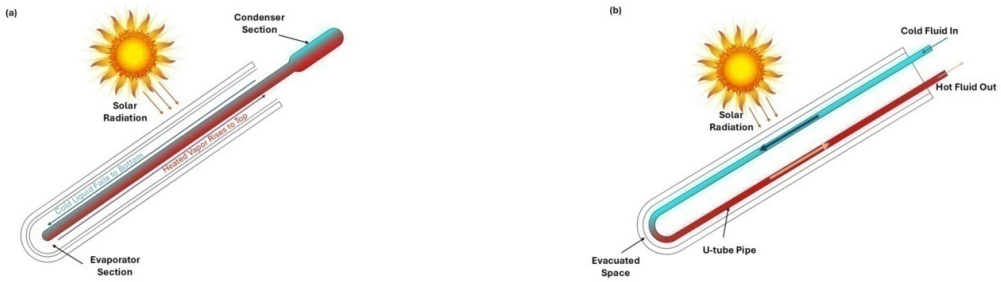

Figure 3. Schematic of evacuated tube collectors: a. heat pipe, b. direct-flow

ETCs have many advantages over other types of solar collectors, such as FPCs, especially in cooler climates and where higher temperatures are needed. While FPCs are simpler and inexpensive to install, they tend to lose heat, especially at higher temperatures. In such conditions, ETCs with higher levels of vacuum insulation can achieve higher efficiencies. They are therefore an ideal choice for industrial process heat, where higher temperatures than those attainable with FPCs are required. For instance, ETCs are used for industrial processes including preheating boiler feedwater, pasteurization, sterilization, and other processes that require high temperatures. ETCs have evolved in diversity and scale due to their advantages over other collectors. Furthermore, integration with other renewable energy systems, especially photovoltaic (PV) systems, is increasingly common as a result of their modularity, economies of scale, and scalability from small rooftop to larger utility-scale sizes. The technology's global uptake was aided by demonstrations of high specific power and other bifacial benefits of about 5.5% compared to ground-mounted PV systems in desert locations (Thar, Great Indian Desert). This showed the value of site optimisation and technology selection for improved energy generation at high-irradiance, remote sites [14]. Photovoltaic/thermal collectors (PV/T) take advantage of the combined advantages of PV and ETC technologies by simultaneously producing electricity and heat [15]. The heat can be used for domestic hot water, space heating or process heating and the electricity can be used to power local loads or feed into the grid; thus, PV/T systems are better suited to multiple uses of renewable energy. These advances reflect the increasing significance of ETCs as thermal collectors and as components of PV/T hybrid systems, and suggest that a better understanding of the mechanisms of improvement is needed.

While there are many advantages to ETCs, products have limitations. The first is that they are costlier in the initial period. This is due to their complex design and manufacturing process. But they

can make up for the initial cost in the long run due to their high efficiency and suitability in hot climates. The second disadvantage is that it may overheat under certain operating conditions, which may cause damage to the collector components. To ensure the long-term efficiency and cost-effectiveness of ETCs, design and optimisation challenges need to be investigated. The efficiency of the collector can be compromised by thermo-hydro-scale in the tube, particularly in dense water. Research and development are underway to avoid these problems and to find other ways to enhance ETC operation, as described in the Introduction. Despite these drawbacks, the advantages of ETCs in the area of high-efficiency, multi-purpose applications; they have too many applications to be a serious contender in the technology of high-efficiency solar energy collectors.

3. Performance improvement techniques

This section summarizes important inititatives that have been undertaken to enhance the performance of ETCs. Particular attention has been paid to nanofluids on the fluid side, where the inclusion of metal oxide, carbon-based and hybrid nanoparticles improve thermal conductivity and heat convection, making them more desirable for thermal performance. But we have problems with large-scale applications such as agglomeration, viscosity, and instability during long-term operation. Another way to stabilise outlet temperatures and enhance the energy supply is the use of PCMs, which absorb heat in high-irradiance conditions and release heat in low-irradiance conditions, thus stabilising outlet temperatures. Apart from these advantages, PCMs suffer from low thermal conductivity, leakage and the lifespan of PCMs, which require composite preparation and encapsulation techniques. Reflectors and concentrators (e.g., compound parabolic reflectors, diffuse flat reflectors) increase the intensity of the sunlight on the absorber surface, thus improving the energy absorption. But they rely on accurate alignment, shading and coating, which are susceptible to dirt, which may reduce their effectiveness. Other design enhancements, such as twisted-tape inserts, grooved tubes and selective coatings, increase turbulence, improve heat transfer and prevent stagnation, but at the cost of higher pressure drop and manufacturing costs. The best performance is achieved when two or more of these techniques are hybridised; that is, they have a complementary effect by minimising thermal losses and exploiting their shortcomings. All these approaches represent the adaptability of ETCs and reflect their robustness in providing medium-temperature heat to devices that provide domestic hot water and industrial process heat, with emphasis on cost, lifespan and ease of installation.

3.1. Utilization of nanofluids

The working fluid in ETC absorbs, transfers, and transports heat, affecting the performance and efficiency of the system. Traditional working fluids, including water, ethylene glycol, and water-ethylene glycol mixtures have been employed in solar thermal systems. These fluids have low thermophysical properties, particularly thermal conductivity, which hampers heat transfer and collector efficiency. The development of nanofluids as advanced working fluids for ETC has been studied in detail to eliminate these shortcomings, leading to enhanced thermal efficiency and heat transfer. Nanofluids are new types of engineered HTFs that are suspensions of nanoparticles (1-100 nm) in conventional base fluids. These colloid suspensions have greater thermo-physical properties (thermal conductivity, heat capacity, and convective heat transfer coefficient) than the base fluids [16]. Various nanoparticles have been investigated for solar thermal applications, such as metal oxides, metals, carbonaceous materials (such as carbon nanotubes and graphene), and hybrid nanoparticles as shown in Table 1.

Sabiha et al. [17] pioneered experimental studies of Single-Walled Carbon nanotube-water suspensions at volume concentrations of 0.05-0.2% and nanotube diameters of 1 to 2 nm, and found a maximum thermal efficiency of 71.84% over pure water at mass flow rate of 0.025 kg/s for heat-pipe ETC in Kuala Lumpur climate. Iranmanesh et al. [18, 19] have furthered this approach by using graphene nanoplatelets (5 to 10 nm) in distilled water at weight concentrations of 0.025-0.1% in a closed-loop heat-pipe ETC, compliant with ASHRAE 93-2003 standards; their findings have shown a thermal efficiency of 90.7% (36% above water baseline), exergy efficiency of 91% (20.5% above baseline), and significant reductions in entropy generation and pumping power requirements. Daghigh and Zandi [20] evaluated Multi-Walled Carbon nanotube, CuO, and TiO_2 at 0.1 %vol in water, with an additional gas in the heat-pipe ETC; their combined experimental-theoretical analysis in Sanandaj, Iran, found collector efficiency gains of 25% for MWCNT, 12-15% for CuO and 5-7% for TiO_2 compared to water, and fuel savings of 67.7% (August) and 42.2% (October). Eidan et al. [21] pioneered acetone-based nanofluids; Al_2O_3 and CuO at 0.25 %vol and 0.5 %vol, with particle sizes of 20 nm and 25 nm in a GAHP-HP-ETC with 70% filling ratio and 45° inclination, reporting thermal performance improvements of 20-54% and efficiency enhancements of 15-38%.

López-Núñez et al. [22] performed numerical computational fluid dynamics analyses in ANSYS-Fluent on water-in-glass ETC using TiO_2 and SiO_2 nanofluids (0.5 %vol, 21 nm & 30 nm), varying solar irradiance and flow rates; TiO_2 nanofluids displayed thermal efficiency enhancements of 24.5% under low radiation and 6.9% under high radiation, exergy efficiency gains of 160% (low) and 26.6% (high), and entropy generation reductions up to 79%, whereas SiO_2 proved less effective under intense irradiation. Khudair and Hussein [23] experimentally probed MWCNT/deionized water nanofluids (0.01-0.05 %vol, purity ≥ 99%) in a heat-pipe ETC at flow rates up to 3 L/min in Al-Hilla, Iraq; they recorded a maximum efficiency enhancement of 69.63% at 0.05 %vol and 3 L/min, and a ΔT increase of 86.84% at 0.05 %vol and 1 L/min. Al-Abayechi et al. [24] used Simcenter STAR-CCM+ to numerically evaluate Al_2O_3/water nanofluids in a U-tube ETC, observing thermal efficiency increases from 58.79% (base fluid) to 60.99% (nanofluid), outlet temperature rises from 44.3-74.8°C (base fluid) to 49.6-80.3°C (nanofluid) and water velocity increases from 0.01 to 0.07 m/s. Surve [25] demonstrated

that graphene-oxide sheets at minute concentrations (0.001-0.003 %vol) in deionized water elevated thermal efficiency from 25.7 (water) to 37.1%; a 44.35% enhancement at 1 L/min in a heat-pipe ETC.

Mahendran et al. [26] reported that TiO_2/water nanofluids(0.3 %vol, 30-50 nm)in a thermosyphonic flow ETC increased efficiency by approximately 16.7% to reach 73%. Ghaderian and Sidik [27] found that Al_2O_3/distilled water(0.03 %vol & 0.06 %vol, 40 nm)nanofluids in a thermosyphonic flow ETC could attain a maximum efficiency of 57.63% at 60 L/h, outperforming water. Sharafeldin and Gröf [28] examined CeO_2/water(0.015-0.035 % vol, 25 nm)nanofluids in a thermosyphonic flow ETC in Budapest, achieving thermo-optical characteristics of up to 34%, ΔT enhancements of 37.3%, and heat gain increases of 42.3%. Yurddaş [29] experimentally and numerically optimized U-type ETC with MWCNT, SiO_2, TiO_2, and Cu nanofluids in the volumetric ratio of 0.5-5%, and concluded that Cu/water nanofluid had the best heat transfer enhancement of 14.09% at 5 %vol. Hosseini and Dehaj [30] compared the performance of TiO_2 nanowires to nanoparticles (1 %vol, 30 nm & 54 nm) in a U-type ETC, achieving thermal efficiency enhancements of 21.1% and 12.2%, respectively. Shahi et al. [31] simulated numerically single-ended thermosyphonic flow ETC with Cu/water nanofluids (up to 0.05 %vol, 100 nm), and demonstrated performance maxima at tilts of 35° and greater gains for higher tilts. Lu et al. [32] experimentally demonstrated that a CuO/water nanofluid (0.8-1.5 wt%, 50 nm) in thermosyphonic flow ETC exhibited the best heat transfer improvement of 30% at 1.2 wt% and a 60% filling ratio.

Tong et al. [33], combining experimental and numerical analyses in Gwangju, South Korea, assessed MWCNT/water nanofluids (0.2 %vol; up to 0.24 %vol) in enclosed U-pipe ETC, reporting thermal efficiency increases of 4% compared with air-filled systems and HTC enhancements of approximately 8% relative to water, along with annual reductions of 1600 kg CO_2 and 5.3 kg SO_2 for fifty-unit arrays. Kaya et al. [34] conducted ZnO/ethylene glycol-pure water (50:50) at 1-4 %vol in Karabük, Turkey, U-tube ETC with different flow rates and found a peak efficiency of 62.87% at 0.045 kg/s and 3% ZnO, i.e., an increase of 26.42% from the base fluid. Kim et al. [35] conducted theoretical studies on U-pipe ETC with a suite of nanoparticles; MWCNT (0.2 %vol), CuO, Al_2O_3, TiO_2, SiO_2 (3 %vol) dispersed in 20% propylene glycol-water demonstrating that thermal conductivity and efficiency rose with concentration, with MWCNT yielding a 62.8% efficiency increase (10.5% over base fluid) and CO_2 and SO_2 emissions reduced by 103.8-345.3 kg/year and 0.4-1.1 kg/year, respectively.

Mahbubul et al. [36] replicated Sabiha's SWCNT/water system (0.05-0.2 %vol, 1 to 2 nm) in Dhahran, Saudi Arabia, and confirmed an efficiency increase from 56.7% (water) to 66% at 0.2 %vol. Ozsoy and Çorumlu [37] achieved efficiency enhancements of 20.7-40% in heat-pipe ETC using Ag/water nanofluids at a concentration of 20 ppm (~0.002 %vol, 60 nm). Dehaj and Mohiabadi [38] demonstrated that MgO/deionized water nanofluids (0.014% & 0.032 %vol, 74.5 nm) in heat-pipe ETC yield an efficiency of ~10.5%, higher than that of water, with further gains achieved by increasing flow rates and concentrations. Kaya and Arslan [39] numerically compared MgO, Ag, and ZnO in ethylene glycol-water (30:70) at 1-4 %vol in U-pipe ETC, noting a peak efficiency of 68.7% for 4 %vol; Ag/ethylene glycol-water (26.7 % over base fluid), and significant coal usage (855.5 kg/year), CO_2 (2241.4 kg/year), and SO_2 (7.2 kg/year) reductions for thirty-unit installations. Sharafeldin and Gröf [40] returned to thermosyphonic flow ETC with WO_3/water(0.014-0.042 %vol, 90 nm),attaining efficiency improvements up to 72.83%(19.3% above water),heat gain increases of 23%, heat removal factor enhancements of 5-16%, and ΔT rises up to 21%. Yan et al. [41] combined experimental and numerical methods to demonstrate that SiO2/water nanofluids(1-5 wt%, 30 nm)in all-glass thermosyphonic flow ETC significantly enhance thermal conductivity and heat transfer in proportion to the nanoparticle fraction, albeit at the expense of reduced optical transmittance. Jamil et al. [42] numerically optimized TiO_2/water(0.05-1 %vol)thermosyphonic flow ETC in Johor, Malaysia, and the highest thermal enhancement was found at 30° inclination and 0.5 %vol, and concentration is positively correlated with the Nusselt number(Nu).Gan et al. [43] experimentally confirmed that TiO_2/water nanofluids(0.1 & 0.5 %vol, 21 nm)in thermosyphonic flow ETC increase efficiency by 16.5% and reduce entropy generation by 1.23 % at 0.033 kg/s. Saxena and Gaur [44] expanded the system boundary by integrating an ETC with a heat exchanger in Madhya Pradesh, India, using CuO/Demineralized water(0.5%, 40 nm)nanofluids; they observed energy efficiency improvements from 42.39 to 45.12%, exergy efficiency increases from 8.90 to 9.51%, and a doubling of annual cash flow.

Elshazly et al. [45] compared MWCNT, Al_2O_3, and hybrid MWCNT/Al_2O_3 (50:50) in water with 0.005-0.05 wt% concentration, and found the highest thermal efficiency of 73.5% (MWCNT), 60% (Al_2O_3), and 69%(hybrid),and exergy efficiency of 51%(MWCNT),44%(hybrid),and 38% (Al_2O_3), and also determined 20% higher performance of hybrid compared to Al_2O_3. Sathish et al. [46] incorporated Al_2O_3 & SiO_2 (50:50) nanofluids (0.5-2 %vol) into an ETC integrated with a PEM electrolyzer and an organic Rankine cycle in Tamil Nadu, India; this complex system achieved thermal efficiency up to 82.1%, exergy efficiency up to 16.4%, ORC efficiency up to 60.4%, hydrogen production of 3105.6 g (36.25% more than water), and overall system efficiency of 71.3% at 2 %vol. Henein and Abdel-Rehim [47] evaluated MgO & MWCNT hybrid nanofluids (0.02 wt%) in heat-pipe ETC, varying hybrid ratios and flow conditions; they recorded maximum energy efficiency increases of 55.83% and exergy efficiency of 77.14% at a 50:50 hybrid ratio. Shahini et al. [48] applied 3D CFD simulation in ANSYS-Fluent to assess Al_2O_3/water-ethylene glycol nanofluids(0.04-0.06 %vol)in a direct-absorption ETC and achieved efficiencies of 66.68-71.39%, the peak 71.4% being at 0.06 %vol and outlet temperature increases of 22.02 to 30.26 K.

Recent studies have yielded promising results that could enhance the thermal performance of ETCs. An experimentally derived neural-network correlation, obtained through a CVFEM simulation,

demonstrated that Nu increases with the Rayleigh number and decreases with the Hartmann number, rendering it a useful prediction tool for nanofluids [49]. The identical trend modelling, with an error of less than 7%, confirmed the same trends on the fluid side, making them more reliable [50]. The non-uniform magnetic fields applied to Fe3O4 ferrofluids in screw tubes demonstrated higher Nu and temperature homogenization, indicating the benefits of magnetism and geometry [51]. Moreover, backwards-facing step flow numerical computations have shown a maximum enhancement of 300% in local Nu in extra-magnetic and wire configurations [52]. These are not solutions to ETCs per se, but such mechanisms may be included to maximize the collector's efficiency in practice.

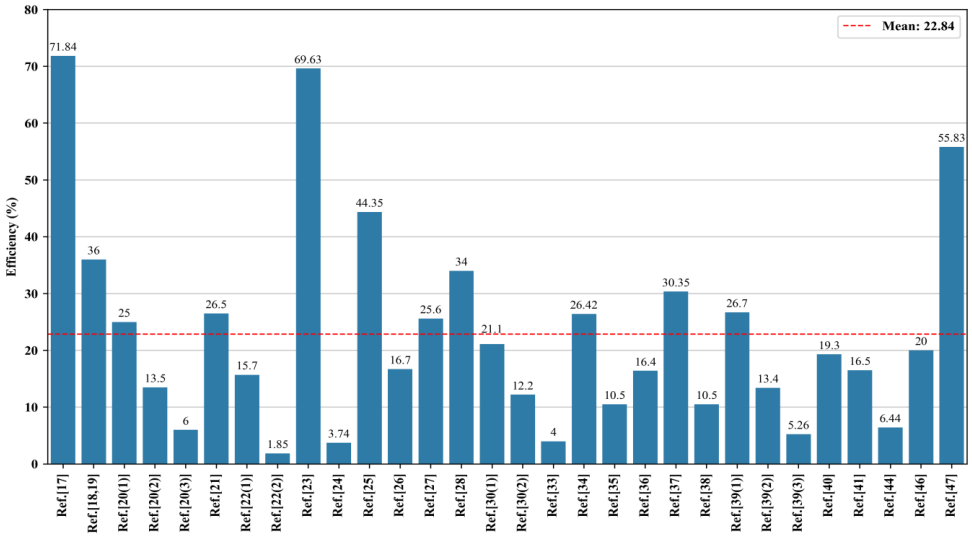

Figure 4. Efficiency enhancement using various nanofluids

The efficiency gains of the reviewed studies that used nanofluids are shown in Figure 4. CNTs and carbon-based hybrid nanofluids significantly enhance the efficiency of ETCs compared with other materials. According to these studies, proper choices of nanoparticle type, concentration, base fluid, ETC configuration, and experimental and numerical methodologies can yield thermal efficiency increases ranging from single-digit percentages to, in some cases, almost doubling baseline performance. Moreover, these methods can simultaneously minimize entropy generation, pumping power, fuel use, and greenhouse gas emissions, thereby facilitating hydrogen and power generation systems. Practical limitations to the use of nanofluids in ETC include limited long-term stability, propensity for agglomeration, risk of abrasion to circulatory-system components, and cost. Zeta-potential, pH control, and ultrasonication regulation are practised to optimal levels to control agglomeration [53]. Surface functionalization and polymeric dispersants, e.g., PVP, would be suspended at high temperatures [54]. Homogeneous suspensions are prepared using methods such as limiting the volume fraction and controlling the flow regime to avoid sedimentation, prevent thermal cycling, and minimise UV exposure [55]. Potentials of zeta more than approximately 30 mV can be maintained for hours to months or longer [56]. Controlled sedimentation can be prevented by dispersion using surfactants, such as sodium dodecylbenzenesulfonate (SDBS) and polyvinyl alcohol (PVP), and by ultrasonication [57]. The pH control and ionic strength can be used to enhance zeta potential with low loadings of less than 0.75 vol%, although very high pH levels are prone to corrosion [58]. Clusters formed through sonication with covalent functionalization or non-ionic surfactants do not form without significantly increasing the viscosity [59]. However, the dynamic viscosity can also increase significantly with increasing particle loading; several-fold increases at specific volume percentages have been reported, and may increase the pumping power and the risk of clogging. Therefore, with the use of particles, it is advisable to adopt low concentrations [60]. Large-scale, long-term outdoor testing of the product under realistic thermal and UV exposure conditions is required to confirm the laboratory findings. Furthermore, hybrid nanofluids also show great potential for ETCs, with heat transfer improvements ranging from 30-45% for MWCNT-Al_2O_3 in oil, 10-22% for TiO_2-Al_2O_3 in EG-water, and 18-35% for Al_2O_3-CuO in water at low concentrations. But long-term stability, deposition and pumping fines limit the use, and the optimal concentration (≤ 0.5 %vol) and stable suspension are essential. Lack of experience and a life-cycle analysis also warrant the need for thermal cycling and UV exposure testing to provide sustainable and scalable ETC operations [61]. Appropriate selection and handling should also be followed to tackle the environmental impact and toxicity of some nanomaterials, to enable sustainable use of these materials.

Table 1. ETCs utilizing nanofluids

Ref.	Nanofluid (material, base fluid, concentration, size)	Methodology highlights	Key performance parameters	Quantitative enhancement
Sabiha et al. [17]	SWCNT/Water, 0.05, 0.1 & 0.2 %vol, 1-2 nm	Experimental; varied vol. concentration & mass flow rates (Kuala Lumpur, Malaysia)	Thermal efficiency	Max thermal efficiency of 93.43% (71.84% enhancement over water implicitly) at 0.025 kg/s
Iranmanesh et al. [18, 19]	Graphene Nanoplatelets (GNP)/ Distilled water, 0.025-0.1 wt%, 5 to 10 nm	Experimental; varied flow rates & GNP mass %; ASHRAE 93-2003 standard (Kuala Lumpur, Malaysia)	Thermal efficiency, Exergy efficiency, Entropy generation	Thermal efficiency up to 90.7% (36% > water), Exergy efficiency up to 91% (20.5% > water), Reduced entropy
Daghigh and Zandi [20]	MWCNT, CuO, TiO_2/ Water, 0.1 %vol	Experimental & Theoretical (Sanandaj, Iran)	Collector efficiency, Fuel consumption saving	MWCNT: Efficiency up by 25%; CuO: Efficiency up by 12-15%; TiO_2: Efficiency up by 5-7% (vs. water), Fuel saving: 67.7% (Aug), 42.2% (Oct)
Eidan et al. [21]	Al_2O_3/Acetone, CuO/Acetone, 0.25 & 0.5 %vol, 20 & 25 nm	Experimental; optimal filling ratio 70% & tilt 45° (Najaf city, Iraq)	Thermal performance, Efficiency	Thermal performance up by 20-54%, Efficiency up by 15-38%
López-Núñez et al. [22]	TiO_2/Water, SiO_2/ Water, 0.5 %vol, 21 & 30 nm	Numerical (CFD, ANSYS-Fluent); varied solar radiation & flow rates	Thermal efficiency, Exergy efficiency, Entropy generation	TiO_2: Thermal efficiency up by 24.5% (low rad.); 6.9% (high rad.), Exergy efficiency up by 160% (low rad.); 26.6% (high rad.), Entropy reduction up to 79% and SiO_2 is less effective at high radiation
Khudair and Hussein [23]	MWCNT/ Deionized water, 0.01, 0.03, 0.05 %vol, Purity ≥ 99 %	Experimental; varied flow rates (Al-Hilla, Iraq)	ΔT, Thermal efficiency	Max efficiency enhancement 69.63% (0.05 %vol, 3L/min), Max ΔT increase 86.84% (0.05 %vol, 1 L/min)
Al-Abayechi et al. [24]	Al_2O_3/Water	Numerical-Simcenter STAR-CCM+ 2022.1 (Baghdad, Iraq)	Outlet temp., Water Velocity, Thermal efficiency	Thermal efficiency 60.99% (58.79% for water), Outlet temp. increased from 44.3-74.8°C to 49.6-80.3°C, Water velocity 0.01 to 0.07 m/s
Surve et al. [25]	Graphene Oxide (GO)/Deionised water, 0.001-0.003 %vol, GO sheets	Experimental; varied flow rates (Ratnagiri, India)	Thermal efficiency	Max thermal efficiency 37.1% (0.003 %vol, 1 L/min) vs. 25.7% for water (44.35% enhancement)
Mahendran et al. [26]	TiO_2/Water, 0.3 %vol, 30-50 nm	Experimental; 2.7 L/min flow rate (Pahang, Malaysia)	Thermal efficiency	Efficiency increased by ~16.7% to 73%
Ghaderian and Sidik [27]	Al_2O_3/ Distilled water, 0.03 & 0.06 %vol, 40 nm	Experimental; varied L/h flow rate (Kuala Lumpur, Malaysia)	Thermal efficiency	Max efficiency of 57.63% (higher compared to water) for 0.06 %vol of nanofluids and a mass flow rate of 60 L/h
Sharafeldin and Grof [28]	CeO_2/Water, 0.015, 0.025 & 0.035 %vol, 25 nm	Experimental (Budapest, Hungary)	Thermo-optical characteristic, ΔT, Heat gain	Thermo-optical characteristic up to 34%, Max ΔT enhancement 37.3%, Heat gain increase 42.3%
Yurddas [29]	MWCNT, SiO_2, TiO_2, Cu (all with Water), 0.5, 1, 3, 5 %vol ratios	Numerical	Heat transfer	Cu/water nanofluid exhibited the best heat transfer enhancement of 14.09% at a 5% volumetric ratio compared to the others.

Hosseini and Dehaj [30]	TiO_2 nanowires/ Water, TiO_2 nanoparticles/ Water, 1 %vol, 30 & 54 nm	Experimental (Rafsanjan, Iran)	Thermal efficiency	TiO_2 nanowires: Efficiency up by 21.1%; TiO_2 nanoparticles: Efficiency up by 12.2%
Shahi et al. [31]	Cu/Water, 0-0.05 %vol, 100 nm	Numerical	Thermal performance, Inclination angle	Nanoparticle inclusion boosts performance, with optimal heat transfer at 35° and stronger effects at steeper angles.
Lu et al. [32]	CuO/Water, 0.8-1.5 wt%, 50 nm	Experimental	Thermal performance, Filling ratio	Optimal 1.2 wt% CuO nanofluid at 60% filling ratio enhances heat transfer by 30%
Tong et al. [33]	MWCNT/Water 0.2 %vol (max 0.24 %vol)	Experimental & Numerical (Gwangju, S. Korea)	Thermal efficiency, HTC	Efficiency up by 4% vs. air-filled system, HTC up by ~8% vs. water, CO_2 & SO_2 emissions down by 1600 & 5.3 kg/year (50 units)
Kaya et al. [34]	ZnO/Ethylene glycol-Pure water (50:50); 1-4 %vol, 30 nm	Experimental; different flow rates & concentrations (Karabük, Turkey)	Thermal efficiency	Max efficiency 62.87% at 3.0 %vol ZnO & 0.045 kg/s; 26.42% up over base fluid
Kim et al. [35]	MWCNT (0.2 %vol), CuO, Al_2O_3, TiO_2, SiO_2 (3 %vol)/ 20% Propylene glycol-Water, 1-100 nm	Theoretical (Gwangju, S. Korea)	Thermal conductivity and Efficiency	Thermal conductivity increased as the concentration of nanofluid increased, Efficiency up by 62.8% with MWCNT (10.5% up vs. base fluid), CO_2 reduction by 103.8-345.3 & SO_2 reduction by 0.4-1.1 kg/year
Mahbubul et al. [36]	SWCNT/ Water, 0.05, 0.1, & 0.2 %vol, 1-2 nm	Experimental (Dhahran, Saudi Arabia)	Thermal efficiency	Efficiency rise from 56.7% (water) to 66% (0.2 %vol SWCNT)
Ozsoy and Corumlu [37]	Ag/Water, 20 ppm (~0.002 %vol), 60 nm	Experimental (Isparta, Turkey)	Thermal efficiency	Efficiency increased by 20.7-40% vs. pure water
Dehaj and Mohiabadi [38]	MgO/Deionized water, 0.014 & 0.032 %vol, 74.5 nm	Experimental (Rafsanjan, Iran)	Thermal efficiency, Flow rate impact	Higher efficiency with MgO (~10.5% vs. base fluid); improve further with higher flow rate & concentration
Kaya and Arslan [39]	MgO, Ag & ZnO/Water-Ethylene glycol (30:70), 1-4 %vol	Numerical (Karabük, Turkey)	Thermal efficiency	Max efficiency: 68.7% for 4 %vol Ag/EG-PW (26.7% increase over base fluid), Coal usage reduction: 855.5 kg/year; CO_2: 2241.4 kg/year; SO_2: 7.2 kg/year (30 units)
Sharafeldin and Grof [40]	WO_3/Water, 0.014, 0.028 & 0.042 %vol, 90 nm	Experimental (Budapest, Hungary)	Efficiency (thermal-optical), Heat gain, ΔT, F_R	Efficiency improved up to 72.83% (19.3% over water), Heat gain increased by 23%, F_R improved by 5-16%, and ΔT up to 21% higher than the base fluid.
Yan et al. [41]	SiO_2/Water, 1, 3 & 5 wt%, 30 nm	Experimental & Numerical (Inner Mongolia, P.R. China)	Thermal conductivity, Heat transfer	Higher SiO_2 nanoparticle fractions (5 wt% > 3 wt% > 1 wt%) markedly raise thermal conductivity and solar-collector heat transfer, albeit at the cost of reduced optical transmittance.
Jamil et al. [42]	TiO_2/Water, 0.05- 1 %vol	Numerical (Johor, Malaysia)	Thermal performance, Inclination angle, Nu	Maximum thermal enhancement occurs at a 30° inclination and 0.5% vol due to the strong thermosyphon and gravity effects; Nu increases with concentration.
Gan et al. [43]	TiO_2/Water, 0.1 & 0.5 %vol, 21 nm	Experimental (Kuala Lumpur, Malaysia)	Thermal efficiency, Entropy generation	16.5% rise in efficiency, whereas 1.23% drop in entropy generation at a corresponding mass flow rate of 0.033 kg/s; heat transfer enhanced by TiO_2 nanofluid
Saxena and Gaur [44]	CuO/ Demineralized water, 0.5 % concentration, 40 nm	Experimental (Madhya Pradesh, India)	Energy and Exergy efficiency, Economic performance	Energy efficiency improved from 42.39% (DM water) to 45.12% (CuO nanofluid), Exergy efficiency from 8.90% to 9.51%, and the annual cash flow doubled

Elshazly et al. [45]	MWCNT, Al_2O_3, Hybrid MWCNT/Al_2O_3 (50:50)/ Water, 0.005-0.05 (wt%), MWCNT: 10–40 nm, Al_2O_3: <30 nm	Experimental	Thermal and Exergy efficiency	Max thermal efficiency: 73.5% (MWCNT), 60% (Al_2O_3), 69% (Hybrid), Exergy efficiency: 51% (MWCNT), 44% (Hybrid), 38% (Al_2O_3); hybrid offered 20% boost over Al_2O_3
Sathish et al. [46]	Al_2O_3 & SiO_2 (50:50)/Water, 0.5-2 %vol, Al_2O_3: 5-20 nm, SiO_2: 25-30 nm	Experimental (Tamil Nadu, India)	Thermal and Exergy efficiency, ORC efficiency, Hydrogen production, Overall system efficiency	Max thermal efficiency: up to 82.1%, Exergy efficiency: up to 16.4%, ORC efficiency: up to 60.4%, Hydrogen production: max 3105.6 g (36.25% more than water), Overall efficiency: 71.3% at 2 %vol
Henein and Abdel-Rehim [47]	MgO & MWCNT (Hybrid)/Water, 0.02 wt%	Experimental; varied hybrid weight ratios & flow rates	Energy and Exergy efficiency	Max energy efficiency increase: 55.83%, Max exergy efficiency: 77.14% (at 50:50 ratio)
Shahini et al. [48]	Al_2O_3/Water-Ethylene glycol, 0.04 & 0.06 %vol	Numerical (3D CFD in ANSYS-Fluent)	Collector efficiency, Outlet temp.	Efficiency: 66.68-71.39%; Max efficiency 71.39% (at 0.06% Al_2O_3/water), ΔT_{out}: 22.02 K (at 0.04% Al_2O_3/water) to 30.26 K (at 0.06% Al_2O_3/EG); Max ΔT_{out} 30.26 K (at 0.06% Al_2O_3/EG)

3.2. Integration of phase change materials

The integration of phase change materials into ETCs is a step towards higher efficiency and overcoming the variable nature of solar radiation. PCMs are materials that store heat during the melting process and release heat during the solidification process. This characteristic allows ETCs with PCMs to store and release thermal energy during the periods of high, low and zero irradiance, thus offering a reliable and consistent energy source. PCMs can be categorised into three main groups: organic (e.g., paraffins, fatty acids, polyethylene glycols), inorganic (e.g., salt hydrates, pure salts) and polymeric or solid-solid systems. Various engineering approaches such as encapsulation, shape-stabilization and composite formation have been proposed to enhance containment, thermal stability and cycling stability [62]. Organic PCMs, inorganic hydrated salts and composite or encapsulated PCMs are the most common PCMs used in thermo-solar applications, as shown in Table 2.

Papadimitratos et al. [63] introduced a dual-PCM system combining Tritriacontane (melting at 72°C, latent heat 256 kJ/kg) and erythritol (melting at 118°C, latent heat 340 kJ/kg) by immersing a heat pipe directly in the PCM contained within the evacuated tube. In their experimental comparison of normal versus on-demand operation modes, the normal mode yielded a 26% increase in collector efficiency, while the on-demand mode produced a 66% increase in collector efficiency. Chopra et al. [64] embedded stearic acid (melting at 67.10°C, latent heat 244.21 J/g) inside heat pipes of a heat-pipe ETC and evaluated daily thermal efficiency across flow rates of 8-20 L/h in Jammu and Kashmir, India. The PCM-integrated system outperformed the base case by 32-37% on a daily basis, achieving efficiency ranges of 79.98-87.8% compared with 42.42-55.46% without PCM integration. Feliński and Sekret [65] examined technical grade paraffin (melting at 58°C, latent heat 217.6 kJ/kg) placed inside all-glass evacuated tubes serving both as collector and storage; through combined experimental and simulation methods in Czestochowa, Poland, they reported charging efficiencies between 33-66%, a 20.5% increase in annual solar fraction, and useful heat gains 45-79% higher than the without PCM baseline.

Abokersh et al. [66] investigated the charging of paraffin wax (melting point: 58-62°C, latent heat: 189 kJ/kg) in direct-flow evacuated tubes with and without fins in Cairo, Egypt. The unfinned collector exhibited 14% higher charging efficiency than the finned version, while the latter showed greater overall energy discharge, highlighting the trade-off between charging and discharging efficiencies. Sheng Xue [67] investigated the inclusion of crystalline hydrate barium hydroxide octahydrate and barium carbonate(melting at 81.83°C, latent heat 193 kJ/kg)within all-glass ETC and found that high PCM viscosity and low thermal conductivity limited performance; nonetheless, constant-flow tests showed a 20% higher efficiency than conventional solar water heaters. Feng et al. [68] conducted numerical parametric studies on U-tube ETC embedded with RT-40(melting range 35-50°C, latent heat 120-250 kJ/kg),demonstrating that lowering the melting point to 35°C boosted efficiency, that an optimal latent heat of 160 kJ/kg maximized performance, and that increased PCM thermal conductivity further improved thermal output. Yong-Li et al. [69] integrated experiment and simulation approaches in Shaanxi, China, employing a composite paraffin/expanded graphite with melting temperature of 69.85°C and latent heat of 200 kJ/kg in U-type ETC; the reduction was 7.4 K in HTF outlet temperature for a PCM with lowered melting temperature of 49.85°C, thermal efficiency of 50.72%, and storage efficiency of 19.2%, as larger tube diameters provided additional efficiency improvements.

Said et al. [70] performed ANSYS Fluent simulations on a U-tube direct-flow ETC containing three PCM: RT 82 (350.15-358.15 K, latent heat 176 kJ/kg), paraffin wax (330.25-334.34 K, latent heat 182.4 kJ/kg), and stearic acid (331-337 K, latent heat 186.5 kJ/kg).

The RT 82 PCM proved most effective, yielding a 9.27% energy gain over the system without PCM. Pathak et al. [71] filled the annular space between the evacuated tube and finned heat pipe with palmitic acid (melting point: 61.10-64.70°C, latent heat ≈: 205 kJ/kg) and evaluated daily useful energy and exergetic efficiencies during clear and cloudy days at a flow rate of 20 L/h in Jammu, India. On clear days, the system delivered 10.65 MJ of useful energy, achieved a next-morning water temperature of 45.2 °C, and had energetic and exergetic efficiencies of 76.57% and 2.37%, respectively. In contrast, on cloudy days, the system yielded 8.52 MJ of energy, a water temperature of 41.4°C, an energetic efficiency of 79.64%, and an exergetic efficiency of 1.38%. Essa et al. [72] placed paraffin wax(54-57°C, latent heat 189 kJ/kg)around U-tubes in a direct-flow ETC in Zagazig, Egypt; varying flow rates revealed a maximum efficiency gain of 21.9% at 0.25 L/min, a drop of 12.2% at 0.35 L/min, and a 6.87% gain at 1.2 L/min, with extended hot-water delivery at lower flow rates. Bazri et al. [73] employed three paraffin waxes(PCM A: 53-57°C, 163 kJ/kg; PCM B: 55-57°C, 260 kJ/kg; PCM C: 70-74°C, 159 kJ/kg)in the manifold of a heat-pipe ETC and conducted MATLAB-based numerical analysis under sunny and cloudy conditions in Kuala Lumpur, Malaysia. They establish system efficiency of 36-54%(sunny)and 47-58%(cloudy)relative to the 40% ±3(sunny) and 32-42%(cloudy)baseline, and determine PCM B to be delivering 25-58% efficiency improvements.

Naghavi et al. [74] conceptualized the operation of a heat-pipe ETC with paraffin wax (64°C, latent heat 174 kJ/kg) incorporating a finned heat exchanger and condenser through a manifold tank in Kuala Lumpur. They estimated that thermal efficiency would be sustained at 55-60% across different flow rates, thereby negating the baseline reduction in efficiency observed in the absence of PCM. Chopra et al. [75] experimentally assessed a stearic acid-integrated manifold heat-pipe ETC in Jammu, India, across multiple mass flow rates; the novel manifold design achieved a maximum thermal efficiency of 72.52% at 24 L/h (approximately 10% higher than conventional designs), PCM efficiencies of 61-64%, and an estimated payback period of six years. Fang et al. [76] utilized a microencapsulated n-octadecane slurry (50 % v/v, melting at 26-30.8°C, latent heat 47.7-52.6 J/g) as the working fluid in a solar simulator-tested heat-pipe ETC (Mazdon TMA600s) in Nottingham, UK, demonstrating collector efficiency of 60-80%, with approximately 76% efficiency at temperature less than 4°C compared to 72% for water, and noted efficiency reductions with higher ΔT/G ratios, prompting modified test methods for accuracy. Wu et al. [77] filled an oscillating heat pipe-based storage ETC with 44 kg of paraffin wax (48-50°C, latent heat 234 kJ/kg) in Nanjing, China, reporting that efficiency fluctuations were reduced by 73% under strong solar and 46% under weak solar conditions, that weak-solar heat output increased by 13.5%, that average collecting efficiency improved by 0.15 during winter, that coefficient of performance (COP) rose from 1.55 to 3.18 at night, and that heating time to 55°C was cut by 130 min.

Pawar and Sobhansarbandi [78] conducted CFD modeling validated by experiments on a heat-pipe ETC with Tritriacontane paraffin(72°C, latent heat 256 kJ/kg)directly filled inside glass tubes in Texas, USA; they reasserted Papadimitratos's findings of 26% efficiency improvement in normal operation and 66% in stagnation, with evening temperature differentials up to 30°C, and achieved close agreement between simulations and experimental data. Alshukri et al. [79] compared paraffin wax grade-A evacuated-tube PCM(64°C, latent heat 268 kJ/kg)and medical paraffin wax PCM(45°C, latent heat 190 kJ/kg)integrated inside tubes and in two external tanks of a gravity-assisted heat-pipe ETC in Najaf, Iraq. Their experiments at 1 L/h and 2 L/h demonstrated that combined tube-and-tank integration yielded a 55.7% efficiency gain over the system without PCM, compared with 49.9% for pure tube integration and 36.5% for tank-only integration. Bin Li and Zhai [80] experimentally and numerically assessed a composite PCM of erythritol plus 3% expanded graphite (melting at 118.69°C, latent heat 312.2 kJ/kg) in aluminium tubes within heat-pipe ETC, finding storage efficiencies of 40.17% at 80°C and 55.24% overall, a 241.4% increase in PCM thermal conductivity over pure erythritol, and heat storage up to 5.17 MJ/m² on days with 12.88 MJ/m² solar irradiance, with performance improving at higher irradiance and smaller tube diameters. Bai et al. [81] tested a modified paraffin (40-60°C, latent heat 238.2 kJ/kg) in all-glass evacuated tubes in Baotou, Mongolia, achieving 97% heat dissipation efficiency at 18°C ambient and 6 m/s airspeed with 414 W dissipation rate, identifying optimal tilt angles of 60° in midsummer and storage efficiency of 55% at 998 W/m² solar radiation. Khan et al. [82] experimented with 3.5 kg of acetanilide as PCM in the annular space of a double-walled, silver solar cooker coupled to a heat-pipe ETC, using various HTFs in Delhi, India. They found that SigmaTherm-K with PCM stored 29.11% more energy than water. Additionally, insulation raised the PCM's peak temperature by 16.5°C with water and by 19.3°C with SigmaTherm-K, compared to the non-insulated case. Although the ETC was not directly examined in the study, the illustrated principles are applicable and may further improve its efficiency. Raj et al. [83] experimentally analyzed 0.70 × 0.90 m² basins from May 2016 to April 2017 using stone chips, sandstone, and a CaO/water exothermic module. The MSS3 (CaO) configuration increased average daily distillate production by 26.98%, which was attributed to higher transient thermal storage and evaporation-driving temperatures.

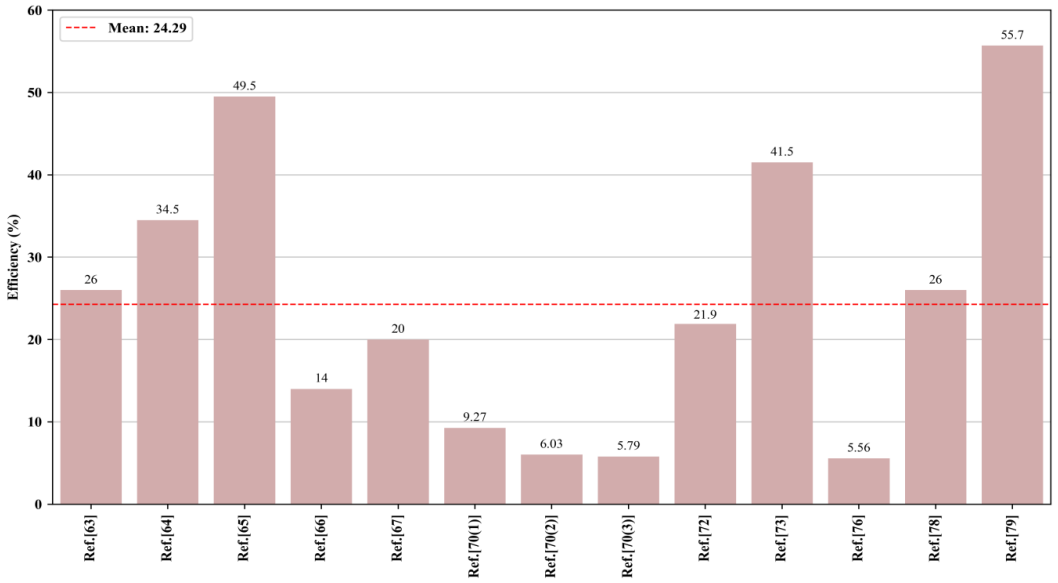

Figure 5. Efficiency enhancement using different PCMs

The efficiency improvements from the reviewed studies with PCMs are shown in Figure 5. The use of paraffin-based PCMs enhanced thermal storage and provided output stability under different weather conditions; the designs with PCMs in manifolds, tubes or tanks showed significant improvements. However, PCMs suffer from low thermal conductivity, leakage, expansion and supercooling. These issues have been addressed by researchers using composite PCMs with conductive fillers, improved encapsulation techniques, and chemical additives. The efficiency gains of the studies reported in this review using PCMs are shown in Figure 5. Paraffin-based PCMs enhanced thermal energy storage and provided stable performance under different weather conditions; the use of PCMs in manifolds, tubes or tanks showed significant improvements. However, PCMs exhibit issues like low thermal conductivity, leakage, expansion, and supercooling. These issues have been tackled by researchers with composite PCMs containing conductive fillers, improved encapsulation techniques and chemical stabilisers. Long-term stability now ranks as the single most critical parameter to influence PCM viability since repeated melting and solidification cause approximately 15-20% volume change, induce supercooling, and result in measurable enthalpy loss, where the values reported are around 126 kJ/kg for microencapsulated paraffin and as high as 350 MJ/m^3 for salt hydrates, thus impairing storage efficiency [84]. Natural PCMs, such as paraffins and acetamide, exhibited substantial thermal stability, ranging from several hundred to over 1,000 cycles, as indicated by cycling performance tests. However, normal degradation parameters need to be established for lifecycle analysis [85]. For the proper functioning of ETCs, PCMs must be chosen based on matching melting points within the operating temperature range, the quality and endurance of encapsulation, and cycle life verification by differential scanning calorimetry and enthalpy change testing, as these factors directly affect system longevity and reliability [86]. Latent-heat thermal energy storage test units utilizing a 60 mm spherical capsule array are discovered to be able to demonstrate that melting time is reduced by approximately 10-30% and solidification time by 14-28% by raising heat transfer fluid flow rate from 1 L/min to 5 L/min; however, at the cost of exergy trade-offs and efficiency reduction at higher flow rates [87]. Within the low-to-moderate range temperature, organic eutectic PCMs of fatty acid/polyethylene glycol mixture provide the option of tunability of melting points from 27-75°C and latent heats of 127-210 kJ/kg, but are not convenient and need compositional adjustment and nucleating agents added to prevent supercooling and attain thermal stability in cycles [88]. Nano-enhanced PCMs like paraffin with CuO nanoparticles were reported to enhance thermal conductivity, stabilize the surface temperature during phase change, and suppress supercooling, whose performances were confirmed through DSC, TGA, and FTIR analysis [89]. In addition to metal oxide additives, zero- to three-dimensional carbon nanostructures exhibit two advantages: phonon-assisted conduction and photon capture, which provide improved charging rates, enhanced effective thermal conductivity, and enhanced solar-to-thermal conversion. However, practical constraints remain in terms of dispersion uniformity, volumetric storage density, and scalability [90]. Together, these results demonstrate that a synergistic strategy involving smart PCM selection, micro- or meso-encapsulation, addition of conductive fillers, and incorporation of photothermal-active carbon is necessary to strike a balance between high storage density and rapid heat exchange. Environmentally friendly, biodegradable, and non-toxic alternatives to PCMs are increasingly important for achieving sustainability in ETC applications.

Table 2. ETCs utilizing PCMs

Ref.	PCM type (material, melting temp., latent heat)	Integration method	Methodology highlights	Key performance parameters	Quantitative enhancement
Papadimitratos et al. [63]	Tritriacontane, 72°C, 256 kJ/kg & Erythritol, 118°C, 340 kJ/kg	Heat pipe immersed in PCM within an evacuated tube	Experimental	Efficiency	Normal operation: 26% efficiency gain; Stagnation mode: 66% efficiency gain
Chopra et al. [64]	Stearic acid (SA-67), 67.10°C, 244.21 J/g	Integrated within heat pipes	Experimental; varied flow rates (J&K, India)	Daily thermal efficiency	Daily efficiency 32-37% higher than no-PCM system; Max-Min daily thermal efficiency 87.8-79.98% (PCM) vs. 55.46-42.42% (w/o PCM) at 20-8 L/h
Felinski and Sekret [65]	Technical grade paraffin, 58°C, 217.6 kJ/kg	Inside evacuated tubes	Experimental & Simulation (Czestochowa, Poland)	Charging efficiency, Annual solar fraction, Heat gain	Charging efficiency: 33-66%, Annual solar fraction increased by 20.5%, Delayed heat release; useful heat gain 45-79% higher
Abokersh et al. [66]	Paraffin wax, 58-62°C, 189 kJ/kg	Inside evacuated tubes	Experimental (Cairo, Egypt)	Collector efficiency, Energy discharge	Collector efficiency without a fin was 14% higher during charging. Finned tube had a higher total energy discharge.
Sheng Xue [67]	$Ba(OH)_2{\cdot}8H_2O$ & $BaCO_3$, 81.83°C, 193 kJ/kg	Inside the vacuum tube	Experimental	System performance and Efficiency	Inferior performance compared to conventional SWH due to the high viscosity and low thermal conductivity of PCM, the system efficiency of the constant flow test is 20% higher.
Feng et al. [68]	RT-40, 35-50°C, 120-250 kJ/kg	PCM embedded in the evacuated tube	Numerical (Hong Kong, China)	PCM (melting point, enthalpy and thermal conductivity), Efficiency	A reduced melting point (50-35°C) enhances efficiency. The latent heat of 160 kJ/kg showed the best performance. Increased thermal conductivity enhanced thermal energy output
Yong-Li et al. [69]	Paraffin/Expanded graphite composite, 69.85°C, 200 kJ/kg	PCM embedded in a vacuum tube	Numerical & Experimental (Shaanxi, PR China)	HTF temp. reduction, Thermal efficiency, Storage efficiency	Reduction of HTF temp. by 7.4 K (at PCM with melting point of 49.85°C), Thermal efficiency 50.72%, Storage efficiency 19.2%, Enlarging the glass tube increases efficiency
Said et al. [70]	RT 82 (350.15-358.15 K, 176,000 J/kg) Paraffin wax (330.25-334.34 K, 182,400 J/kg) Stearic acid (331-337 K, 186,500 J/kg)	PCM inserted in the evacuated tube	Numerical (ANSYS Fluent)	Energy gain	RT 82 most suitable: energy gain of 9.27% vs. w/o PCM. The system (PTSC+PCM+fins) achieved a 42.94% energy efficiency gain.
Pathak et al. [71]	Palmitic acid, 61.10-64.70°C, 204.93-205.52 kJ/kg	PCM filled in the annular space between the evacuated tube and the aluminium finned heat pipe	Experimental; 20 L/h flow rate (Jammu, India)	Daily useful energy, Stored water temp.. Daily energetic & exergetic efficiency	Clear day: 10.65 MJ energy, 45.2°C next morning, η_{en}76.57%, η_{ex} 2.37%; Cloudy day: 8.52 MJ, 41.4°C, η_{en}79.64%, η_{ex} 1.38%
Essa et al. [72]	Paraffin wax, 54-57°C, 189 kJ/kg	PCM placed around U-tubes in evacuated tubes	Experimental; varied flow rates (Zagazig, Egypt)	System efficiency	Efficiency gain: 21.9% (at 0.25 L/min); efficiency drop: -12.2% (at 0.35 L/min); efficiency gain: 6.87% (at 1.2 L/min), and longer hot water supply at lower flow rates
Bazri et al. [73]	3 Paraffin wax: PCM A: 53-57°C, 163 kJ/kg PCM B: 55-57°C, 260 kJ/kg PCM C: 70-74°C, 159 kJ/kg	PCM filled in the manifold	Numerical-MATLAB (Kuala Lumpur, Malaysia)	System thermal efficiency	New system efficiency: 36-54% (sunny), 47-58% (cloudy); Baseline: 40% ±3 (sunny), 32-42% (cloudy); Best PCM B shows a 25-58% enhancement over the baseline.

Naghavi et al. [74]	Paraffin wax, 64°C, 174 kJ/kg	PCM in a manifold tank connected to the collector	Theoretical (Kuala Lumpur, Malaysia)	Thermal efficiency	Efficiency maintained at 55-60% across different flow rates (compared to baseline drop)
Chopra et al. [75]	Stearic acid, 57-60°C, 191 kJ/kg	PCM-integrated manifold	Experimental; different mass flow rates (J&K, India)	Thermal efficiency, PCM efficiency, Payback period	Max thermal efficiency: 72.52% (MDCM at 24 L/h); efficiency is higher under MDCM than FDCM (by ~10%), PCM efficiency: 61-64%, Payback period: 6 years
Fang et al. [76]	Microencapsulated PCM (n-octadecane, PC210), 26-30.8°C, 47.7-52.6 J/g	PCM used as a slurry (50% v/v) in place of water as HTF	Experimental with solar simulator (Nottingham, UK)	Collector thermal efficiency	MPCM suspension showed 60-80% efficiency, ~76% at <4°C vs. 72% (water), with efficiency decreasing as ΔT/G increased and improved accuracy using a modified test method
Wu et al. [77]	Paraffin wax (48#), 48-50°C, 234 kJ/kg	PCM (44 kg) filled in the evacuated tube	Experimental (Nanjing, China)	Collecting efficiency, Average collecting efficiency, Coefficient of Performance (COP), Exit water temp.	Collecting efficiency fluctuation was reduced by 73% (strong solar) and 46% (weak solar); heat output increased by 13.5% in weak solar conditions. Average collecting efficiency improved by up to 0.15 in winter. COP increased from 1.55 to 3.18 during winter nights, and the heating time to 55°C was reduced by 130 minutes.
Pawar and Sobhansarbandi [78]	Tritriacontane paraffin, 72°C, 256 kJ/kg	PCM is directly filled inside the glass tube	CFD modeling; validated with experimental data (Texas, USA)	Thermal performance vs. non-PCM case	Thermal efficiency improved by 26% (in normal operation) and 66% (in stagnation), and the maximum evening temperature difference was 30°C greater than that of the non-PCM system.
Alshukri et al. [79]	Paraffin wax grade-A (ET), 64°C, 268 kJ/kg & Medical paraffin wax (tanks), 45°C, 190 kJ/kg	PCM is integrated both inside the evacuated tube (ET) and in two external tanks adjacent to the water storage tank	Experimental; tested at different flow rates (Najaf, Iraq)	Efficiency	Efficiency gain (vs. w/o PCM): HP/ETC-C (ET + Tanks): +55.7%; HP/ETC-D (ET only): +49.9%; HP/ETC-A (Tanks only): +36.5%
Bin Li and Zhai [80]	Composite PCM: (Erythritol + 3 wt% Expanded graphite), 118.69°C, 312.2 kJ/kg	PCM filled in aluminium tubes inside evacuated tubes	Experimental & Numerical	Thermal performance	Average storage efficiency: 40.17% (at 80°C), 55.24% (total). Thermal conductivity improved 241.4% over pure erythritol. Heat storage up to 5.17 MJ/m² on a day with 12.88 MJ/m² solar irradiance. Storage performance improved with a smaller tube diameter and higher irradiance.
Bai et al. [81]	Modified paraffin, 40-60°C, 238.2 kJ/kg	PCM filled in all-glass evacuated tubes	Experimental (Baotou, Mongolia)	Thermal performance	97% heat dissipation efficiency at 18°C ambient, 6 m/s airspeed and heat dissipation rate: 414 W, Optimum elevation angle: 60° (July/August) and optimal storage efficiency: 55% at 998 W/m² solar radiation
Khan et al. [82]	Acetanilide, 114.3°C	PCM (3.5 kg) filled in the annular space between a double-wall cooking vessel, solar cooker (silver, dia. 200 mm & length 100 mm)	Experimental, using different heat transfer fluids (Delhi, India)	PCM Energy stored & temp.	SigmaTherm-K + PCM stored 29.11% more energy vs. water & Insulated cooker raised PCM temp. by 16.5°C (water) and 19.3°C (SigmaTherm-K) vs. non-insulated

3.3. Incorporation of reflectors/concentrators

The use of reflectors and concentrators is a key method for increasing ETC performance, as they allow a higher percentage of incident solar radiation to be captured and converted into useful heat. Reflectors, usually made of highly reflective material, direct sunlight towards the absorber tube and consequently double the solar flux incident on the absorber tube. Concentrators, however, use lenses or curved mirrors to concentrate sunlight onto a smaller area, resulting in an even higher concentration of sunlight. Several reflector/concentrator geometries have been explored for ETC, each with its own strengths and weaknesses, as illustrated in Table 3.

Schumann et al. [91] investigated diffuse (trapezoidal) and specular (plane) rear-side reflectors, made from galvanized metal sheets and aluminium, respectively, on a heat-pipe ETC in Würzburg, Germany, using ray-tracing (Zemax) and TRNSYS simulations. They showed annual collector output increases of around 30% for diffuse reflectors and 33% for specular reflectors, with an improvement in the system yield of around 11% in both cases, relative to non-reflecting collectors. Subsequently, Altaher et al. [92] deployed horizontal and vertical secondary parabolic trough reflectors, made of polished aluminium foil around heat-pipe bulbs in Aswan, Egypt. They reported that the bulb temperature was increased by about 11% with the addition of a vertical secondary reflector, resulting in a considerable improvement in the heating performance of the collector under hot and dry conditions. Chai et al. [93] applied an inner focusing reflective coating (deposited using magnetron sputtering) of a metal-based film on the bottom half of the outer glass tube with an eccentric inner absorber in an ETC in Shanghai. Through combined experimental work and optical analysis (using TracePro), they found thermal efficiencies ranging from 0.65 to 0.72, approximately 10% higher than those of conventional evacuated tubes, and reductions in heat-loss coefficients of 27-48%. In Assiut, Egypt, Abo-Elfadl et al. [94] compared the use of upper, lower, and dual (upper-lower) glass reflectors in a heat-pipe ETC with PCM storage. Their experimental data and thermal modeling of the tilt angles revealed that dual reflectors increased daily input energy by 37%, daily stored energy by 35.7%, thermal efficiency to 76.25% (from 60.57% without reflectors), and average daily exergy efficiency to 25.3%.

Pourbafrani et al. [95] examined a symmetrical compound parabolic concentrator(CPC)of stainless steel in Alborz, Iran, positioning ETC at the CPC focal point; their passive-circulation study showed that the average energy efficiency climbed to 71.1%; 2.8% above the conventional system, and that single-tube performance under CPC was 2.7 times higher, with tank temperatures elevated by 2.35°C. Sunkarwar et al. [96] experimented with and simulated via CFD a parabolic reflector integrated with a parallel-flow U-tube ETC under dusty conditions, and reported a maximum thermal efficiency of 66% without particulate matter treatment (PMT) and 61% with PMT; the latter's 17% drop highlighted the vulnerability of reflectors to dirt. Morrison et al. [97] validated natural-circulation flow in a water-in-glass ETC with a diffuse flat reflector (DFR) and simulated a parabolic variant, finding that circulation rates peaked at 35 kg/h under 1 kW/m² and 60°C tank conditions and could double when heating the tube's upper half vs. the lower half.

Chen et al. [98] compared a 3D-printed polylactic acid-based CPC(0.87 reflectivity)against a standard all-glass ETC in Kunming, China, and, supported by theoretical modeling, reported thermal efficiency of 66.8% with CPC vs. 53.7% without. Milani and Abbas [99] employed a specular DFR(~0.85 reflectivity)behind active-circulation all-glass ETC arrays in various Australian solar zones; their multiscale simulations predicted performance improvements from 14.6 to 27.9% and energy savings increases of 12-17% depending on the geographic irradiance profile. Budihardjo et al. [100] mounted 21 water-in-glass tubes over a DFR and, through experimental and numerical investigations, showed natural circulation rates of 20-25 kg/h per tube at 45°, which doubled under top heating and remained stable up to 30° transverse incidence. Selvakumar et al. [101] combined an external parabolic trough solar reflector (a stainless steel sheet) with a Therminol D-12-filled fluid-in-glass ETC in India. The experimental tests showed a 30% improvement in thermal efficiency with outlet temperatures up to 68°C (vs. 40°C without the reflector) and no degradation in oil properties after 100 cycles. Wang et al. [102] designed a medium-temperature CPC using smooth aluminium reflectors (0.91 reflectance) with SiO_2 antireflective porous coating of vertical all-glass tubes; their numerical analysis reported an instantaneous thermal efficiency of 50.2% at 150°C. Avargani et al. [103] coupled optical and thermal COMSOL models with experiments on 24 spiral parabolic trough collectors (PTCs) in Iran, establishing that an optimal diameter-to-focal-length ratio (d/f = 0.8) yielded a system efficiency of 70%, compared to under 60% for standard focal-line configurations. Naik et al. [104] compared an evacuated U-tube ETC with and without an external stainless steel parabolic reflector in Assam, India, finding that the enhanced system achieved an average thermal efficiency of 54%, 14.1% higher than the baseline of 46%. However, this improvement came at the cost of increased thermal losses during peak solar hours.

Dinesh et al. [105] compared flat and wavy galvanised iron diffuse reflectors in a passive water-in-glass ETC in Tamil Nadu, India, and found that tank temperatures increased by 4°C with flat reflectors, whereas wavy reflectors achieved up to 6°C increases, 2°C higher than those of flat types. Ma et al. [106] combined a CPC with aluminium reflectors featuring a novel selective coating, aluminium fins, Ni-coated Cu U-tubes, and antireflective glass in a 12-tube array in Jinan, China; over a five-year durability study, they recorded solar absorptance of 0.95 at 80°C, thermal efficiency up to 46% at 150°C, and steam temperatures between 108-145°C. Zambolin and Del Col [107] experimentally compared flat-plate, ETC with external CPC reflectors in Padova, Italy, demonstrating that ETC outperformed flat plates by 3-5% above a thermal resistance factor of 0.037 m^2K/W(≈57°C)and up to 10% in daily efficiency beyond 0.027 m^2K/W(≈39°C).Li et al. [108] evaluated truncated stainless-steel CPC with 3M solar mirror film(0.94 reflectivity)at concentration ratio(CR)of 3.06 and 6.03 on finned U-tube ETC in Shanghai; their

combined theoretical and experimental work reported maximum daily efficiencies of 51%(CR = 3)and 54%(CR = 6)at 150°C, with optical efficiencies of 0.74 and 0.70, respectively. Fathabadi [109] assessed the incremental benefits of parabolic trough reflectors and single/dual-axis trackers on a CuO-H_2O coated heat-pipe ETC in Athens, Greece; theoretical and experimental results indicated efficiencies of 52.3% (ETC alone), 43% with reflector only, 56.3% with reflector plus single-axis tracking, and 58.6% with reflector plus dual-axis tracking. Teles et al. [110] developed an internal reflective film inside an eccentric copper-tube ETC in Brazil. The validated numerical models showed a peak efficiency comparable to that of PTC(~73%), along with improvements in thermal uniformity and reductions in stress. Saadoon et al. [111] installed a 45° flat mirror reflector behind a 30-tube ETC array in Baghdad, Iraq, and experimentally demonstrated daily efficiency gains of +6%, +11%, and +5% over three days (efficiency with reflector: 53%, 39%, 35%; without reflector: 47%, 28%, 30%) and corresponding increases in outlet temperature. Nkwetta et al. [112] carried out 2D ray-tracing calculations on an internal truncated reflector (CR = 1.95, 0.95 reflectivity) of a heat-pipe ETC. They obtained a total optical efficiency of 79.13% and an average acceptance angle of 93.72% (0-20° incidence) and showed the potential of small internal concentrators for solar air-conditioning.

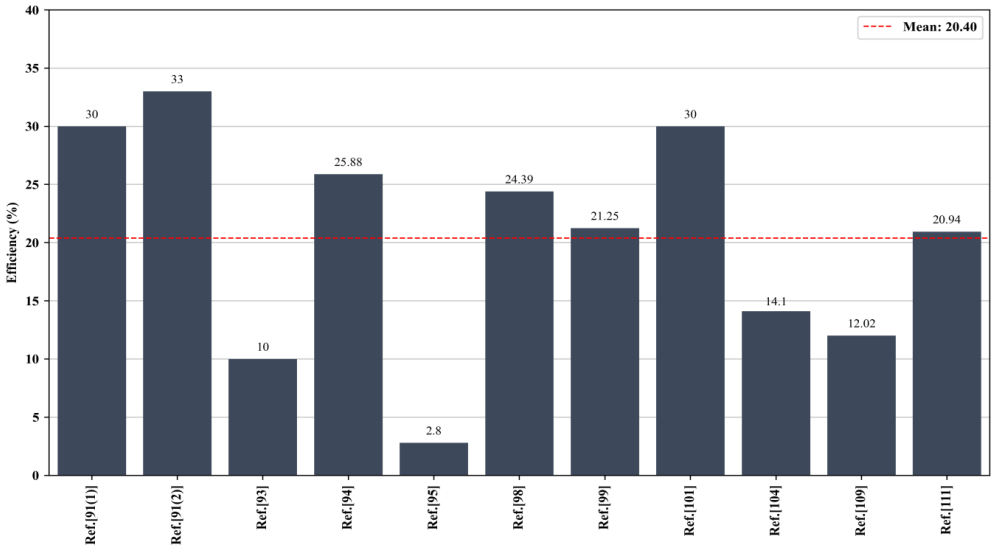

Figure 6. Efficiency enhancement using reflectors/concentrators

Figure 6 shows the gains in efficiency seen in this study with the addition of reflectors and concentrators. The use of diffuse, specular, dual-glass, and parabolic-trough-type reflectors, as well as compound parabolic concentrators, has resulted in a significant improvement in thermal efficiency of the ETC. This is achieved through improvements in solar-energy absorption and conversion efficiencies in various climactic and collector designs. The main drawback is the simultaneous use of reflector and concentrator, which leads to a greater shading effect and higher tracking accuracy demands to ensure optical alignment. Long-term investigations have revealed that reflector-evacuated tube collectors suffer from a range of problems, such as mechanical stress due to wind and snow loads and environmental degradation due to corrosion, soiling and ageing from UV radiation and thermal cycling. This results in long-term structural deformation and mounting tolerance shift [7]. It also suffers from progressive misalignment and deterioration of the reflectors, poor tracker accuracy and different thermal expansion of the components, which results in a loss of incidence angle and transmittance-absorptance efficiency [13]. Optically, non-imaging CPCs are also less sensitive to misalignment and the incidence angle dependence of thermal efficiency is generally less than 10% for low concentration ratios, while specular concentrating reflectors must have much closer optical tolerances for sustained operation [113]. But the benefits of using reflectors or concentrators outweigh the disadvantages, particularly for high-energy and high-temperature applications. The improved thermal efficiency and solar energy conversion efficiency result in not only better collector efficiency but also better economic viability; therefore, reflector/concentrator-based ETCs become more feasible and credible for various solar thermal energy applications.

Table 3. ETCs equipped with reflectors/concentrators

Ref.	Reflector/ Concentrator type & Material	Design/ configuration details	Methodology highlights	Key performance parameters	Quantitative enhancement
Schumann et al. [91]	Diffuse (trapezoidal) vs. Specular (plane), Galvanized metal sheet vs. Aluminium	Rear-side reflectors	Ray-tracing (Zemax) & TRNSYS simulations (DHW system, Würzburg, Germany)	Annual collector output, Annual system yield	Diffuse: ~30% output gain; ~11% system yield gain, Specular: ~33% output gain; ~11% system yield gain
Altaher et al. [92]	Secondary reflector with primary Parabolic trough, Aluminium foil covering polished Al	Horizontal & vertical secondary reflectors on PTSC	Experimental (Aswan, Egypt)	Heat pipe bulb temp.. Collector heating capability	Vertical secondary reflector + Al foil: heat pipe bulb temp. by ~11% vs. reference, improved the heating capability
Chai et al. [93]	Inner focusing reflective coating, Metal-based reflective film (via magnetron sputtering)	Coating on the lower half of the outer glass tube, eccentric inner absorber (180° coating angle optimal)	Experimental & Mathematical model- thermal resistance network, Optical analysis-TracePro (Shanghai, China)	Thermal efficiency, Heat loss reduction	Thermal efficiency: 0.65-0.72 (~10% higher than conventional ETC), Heat loss coefficient reduced by 27-48%
Abo-Elfadl et al. [94]	Upper, Lower, and Upper-Lower (two) reflectors, Glass reflectors	Integrated with the ETC-HP system	Experimental thermal model for reflector tilt angles (Assiut, Egypt)	Input energy, Storage energy, Energy efficiency, Exergy efficiency	Two reflectors: Input energy by 37%, Daily storage energy by 35.7%, Daily thermal efficiency 76.25% (vs. 60.57% w/o reflector), Avg. daily exergy efficiency by 25.3%
Pourbafrani et al. [95]	CPC, Stainless steel	Symmetrical CPC, partial circle shape, ETC, at the focal point	Experimental; comparison with/ without CPC (Alborz, Iran)	Energy efficiency, Tank water temp.	Avg. energy efficiency with CPC: 71.1% (2.8% > conventional); single tube performance with CPC: 2.7 times higher, Tank temp. 2.35°C higher
Sunkarwar et al. [96]	Parabolic reflector	Integrated with a parallel flow evacuated U-tube SC	Experimental & Numerical (CFD); with/ without particulate matter treatment (PMT)	Thermal efficiency	Max thermal efficiency: 66% (no PMT); 61% (with PMT)
Morrison et al. [97]	DFR (baseline) & Parabolic reflector (simulated)	Single-ended water-in-glass evacuated tubes, 1.42 m long, 37 mm diameter, 45° inclined; direct connection to tank; simulations also for parabolic reflector	Experimental validation with particle image velocimetry & CFD modeling using FLUENT (Sydney, Australia)	Circulation rate	Circulation rate of up to 35 kg/h at a 60°C tank temperature. and 1 kW/m² solar input; up to 2 times higher circulation when heat is applied to the top vs. the bottom half of the tube
Chen et al. [98]	CPC, 3D-printed PLA substrate with reflective film (reflectivity = 0.87)	Compared with a standard all-glass ET	Experimental & Theoretical (Kunming, PR China)	Overall thermal efficiency	Experimental efficiency: 66.8% (CPC) vs. 53.7% (w/o CPC)
Milani and Abbas [99]	DFR, Specular DFR with ~0.85 reflectivity	DFR is placed behind the ETC array	Theoretical/ Simulation (Australia)	Performance improvement, Energy savings	Potential performance improvements: 14.6% to 27.9% (depending on Australian solar zone), Energy savings increase: up to 12-17% with DFR

Budihardjo et al. [100]	DFR	21 single-ended water-in-glass evacuated tubes mounted over a diffuse reflector	Experimental & Numerical	Circulation flow rate (Natural circulation)	Flow rate peaked at 20-25 kg/h per tube (3-4 exchanges/hr) at 45°; doubled with top heating and remained stable up to 30° transverse incidence.
Selvakumar et al. [101]	Parabolic trough reflector (External), Stainless steel sheet	Parabolic trough coupled with standard evacuated tube; uses Therminol D-12 oil as HTF; connected to heat exchanger storage tank via passive coil	Experimental	Heating efficiency, Outlet temp.., Thermal stability of HTF	30% higher efficiency with parabolic trough compared to without, Outlet temperature of water: 68°C (with trough) vs. 40°C (without), Therminol properties stable after 100 cycles
Wang et al. [102]	CPC, Smooth aluminium sheet (Reflectance = 0.91)	All-glass vertical tubes, porous SiO_2 AR coating, selective Al/TiAlON/AlON layer, copper U-tubes, 2.7 times CPC	Optimization	Instantaneous solar thermal efficiency	50.2% thermal efficiency achieved at 150°C
Avargani et al. [103]	PTC, Polished stainless steel	24 PTC in spiral box; black copper pipe (1 m); tilt-adjustable; d/f = 0.8; 4 mm glass cover	3D CFD and optical modeling (COMSOL); non-sequential ray-tracing and FEM & experimental validation (Isfahan, Iran)	System thermal efficiency	Efficiency: 70% (optimal d/f = 0.8) vs. <60% (focal line); the location of the absorber pipe with respect to the collector has a significant influence on efficiency
Naik et al. [104]	Parabolic reflector (External), Stainless steel sheet	ETC with/without integrated parabolic reflector (EUSCIPR vs. CEUSC); absorber is copper U-tube inside evacuated glass tube	Experimental & Numerical-Comparison (Assam, India)	Thermal efficiency	Avg. thermal efficiency: EUSCIPR = 54%, CEUSC = 46% -> +14.1% for EUSCIPR; thermal losses were enhanced during the peak hours
Dinesh et al. [105]	Flat and wavy diffuse reflector, Galvanized Iron (GI) sheets with reflective paint	10 borosilicate tubes, 100 L PUF tank, both GI reflectors with CoolCoat, 26° tilt	Experimental (Tamil Nadu, India)	Tank water temp.	Flat reflector increased tank water temp. by 4°C over baseline; wavy reflector improved it by 6°C; wavy outperformed flat by 2°C
Ma et al. [106]	CPC, Aluminium reflector with novel selective coating	12 ETs (dia. 47×1500 mm), CPC reflectors below tubes, Al fins, Ni-coated Cu U-tubes, AR glass, dual getters, modified sealing	Experimental (Jinan, China)	Solar absorptance, Instantaneous efficiency, Thermal performance	Solar absorptance: 0.95 at 80°C, Efficiency: up to 0.46 at 150°C, Steam temp: 108-145°C and long-term stability and durability post-5 years of operation
Zambolin and Del Col [107]	CPC	Direct flow ETC with 21 vacuum glass tubes; CPC reflector integrated externally.	Experimental; comparison with FPC (Padova, Italy)	Efficiency	ETC outperforms flat-plate by ~3-5% above T_m = 0.037 m^2·K/W (≈57°C) and up to ~10% better daily efficiency above $T_{m,day}$ = 0.027 m^2·K/W (≈39°C)
Li et al. [108]	Truncated CPC, Stainless steel substrate with 3M solar mirror film (Reflectivity 0.94)	Two CPC: 3 CR, fixed (CR = 3.06), 6 CR manual 5 times/day (CR = 6.03), both with 1500 mm U-tube finned evacuated tubes in wood molds	Theoretical & experimental validation (Shanghai, China)	Efficiency	Max daily efficiency: 51% (3 CR, CPC); 54% (6 CR, CPC) at 150°C temperature. 3 CR, CPC performs better in the morning/evening (higher IAM), while 6 CR, CPC exhibits higher efficiency at high temperatures. Optical efficiency up to 0.74 (3 CR) & 0.70 (6 CR)

Fathabadi [109]	Parabolic trough reflector	Novel 240 cm TPCT-based ETC with CuO-H_2O nanofluid and NiO coating was tested in four setups: ETC, +reflector, +single-axis tracker, and +dual-axis tracker	Theoretical & Experimental (Athens, Greece)	Thermal efficiency	Efficiency: ETC+R-43%; ETC+R+ST-56.3% (+4% over ETC); ETC+R+DT-58.6% (+6% over ETC); ETC alone-52.3%
Teles et al. [110]	Internal reflective film	Eccentric copper tube in glass cover with reflective film, vacuum insulation, selective surface, Therminol 66, CR~2.08, monthly one-axis tracking	Numerical model; validated with multiple experimental datasets (São Luís, Brazil)	Efficiency	Max efficiency comparable to PTC (73%) and reflective film improved uniformity & reduced thermal stress.
Saadoon et al. [111]	Flat mirror reflector, Two aluminium layers + polymeric core, coated reflective face (84-90% reflectivity)	Two 30-tube ETC with 150 L tank; one with 45° flat mirror (197×125 cm); selective borosilicate tubes; closed-loop flow for testing	Experimental comparison (Baghdad, Iraq)	Thermal performance	Efficiency with reflector: 53%, 39%, 35% (3 days); without reflector: 47%, 28%, 30%; relative gain: +6%, +11%, +5% respectively and increase in temp.
Nkwetta et al. [112]	Truncated reflector (Internal low-concentrating HP), Aluminium sheet-2 mm (0.95 reflectivity)	Internal low-concentrating ETHP collector: truncated half acceptance angle = 20°; CR = 1.95; 3.5 mm borosilicate glass tube (OD/ID = 100/93 mm); 3 mm absorber-reflector gap; 15 mm absorber dia.	2D Ray-tracing simulation (Eazee tool)	Optical efficiency, Angular acceptance	Overall optical efficiency: 79.13% (0-20°), Angular acceptance: 93.72% average (0-20°) and improved irradiance concentration with truncated CPC profile

3.4. Implementation of design alterations

Various design alterations have been studied to enhance the thermal and hydraulic performance of ETC, ranging from internal fin and tape inserts to external shields and bypass tubes, as shown in Table 4. Supankanok et al. [114] inserted stainless-steel scrubber elements, weighing approximately 109.7 g, and occupying a ~2% void fraction between a 58 mm OD glass tube and a 14 mm OD copper heat pipe, using a 10 mol% ethylene glycol-water mixture as the working fluid. Their combined experimental and mathematical model at Ladkrabang, Bangkok, produced a mean outlet fluid temperature rise of ~22°C (160.3°C vs. 138.7°C), a 34.96% increase in efficiency, and a 10-fold improvement in the overall HTC, effectively reducing the number of tubes required by 20% to generate the same thermal output. In central India, Agade et al. [115] evaluated both plain and perforated wavy tape (PWT) inserts; the perforated inserts were fabricated from 0.3 mm copper strips folded at 60° intervals and perforated with equilateral triangles having side lengths of 6 mm and 9 mm, in an eight-tube, 1.5 m² aperture ETC. Their hourly and daily experiments demonstrated that the 6 mm-PWT arrangement achieved a peak hourly efficiency of 83.33%, an average energy efficiency of 49.36%, and an average exergy efficiency of 70.18%, outperforming the no wavy tape (WT), the plain wavy tape, and the 9 mm perforated variant by 27.5%, 9.84%, and 3.5% in energy gains. Yao et al. [116] conducted numerical CFD simulation of twist-tape inserts in a 47 mm ID, 1.8 m long all-glass ETC tube, and discovered that the y = 2.5; reduced the heat transfer by only a small amount (-1.07% Nu number change) and the y = 4; enhanced the Nu by 9.29% under increased fluid temperature, indicating that insert geometry should be designed to suit operating conditions. Generalizing the tape-insert analogy to solar air-heating, Kumar et al. [117] proposed a theoretical model of an evacuated tube with inserted baffles using loose-fit perforated twisted tape (LFPTT) of y/D = 2-3 and d/D = 0.0714-0.143. Their research, conducted at airflow rates up to 400 kg/h, achieved the highest thermal efficiency of 62.33% and the highest exergy efficiency of 3.91% at y/D = 2 and d/D = 0.0714. Optimal performance occurred at lower volumetric flow rates but was accompanied by increased pressure-drop losses.

Said et al. [118] compared a helical coiled thermal exchange tube, comprising 59 turns of 7.94 mm diameter piping over a 700 mm heat transfer length, against conventional heat-pipe, U-tube, double-U-tube, and coaxial direct-flow ETC under a 1000 W/m² solar simulator. The helical tube geometry achieved 69% efficiency, surpassing

the baseline heat pipe (31%) and the 41-54% range observed for the other geometries. This demonstrates that internal helical pipes can nearly double the effectiveness of the collector. Kumar et al. [119] investigated the ETC with inserted baffles in South India by fitting it with axial baffles of different lengths. Using both experimental measurements and analytical modeling across mass flow rates up to 1000 kg/h, they reported a maximum air-temperature rise of 42.8°C, with the lowest thermal efficiency of 35.31% at 100 kg/h, and found that increasing baffle length positively affected temperature rise and thermal efficiency but increased pumping power. Mukuna and Gryzagoridis [120] evaluated five different internal insert profiles (I, V, triangular, square-inserts without insert) in an ETC with a heat-pipe under an indoor simulator of 700 W/m^2 at Durban, South Africa. They concluded that the square profile had the highest dry-mode efficiency (24.4% vs 20.3% without inserts), and that when used with distilled water as the working fluid it recorded an efficiency of 64.3% (vs 53.3% without inserts), suggesting a synergistic effect between fluid choice and insert geometry.

In north India, Singh and Vardhan [121] experimentally introduced helical coiled inserts, wound from 1.5 mm wire at a unit pitch ratio, into a coaxial-flow evacuated tube air heater comprising 20 mm inner and 58 mm outer conduits. Operating at mass flow rates of up to 0.003 kg/s, they achieved a maximum outlet temperature of 112.6°C and a peak efficiency of 70.9%, compared with 64.5% at higher flow rates, despite a 2.45-fold increase in pressure drop. This confirms that coiled inserts can deliver substantial temperature gains without prohibitive costs. Singla et al. [122] applied the CFD to investigate roughening of half a tube absorber for air-heating purposes under the constant relative roughness height e/D = 0.071 and variable pitch P/e = 6-12. At R_e = 8000 and P/e = 10, their findings resulted in a 1.88 times Nu enhancement and a 2.89 times friction factor increase, but a total thermo-hydraulic performance parameter(THPP) of 1.36, which represents a good balance between heat transfer and pumping work. Liang et al. [123] proposed a filled-layer concept, which involves placing a U-tube inside a two-layer glass ETC with a high-conductance absorber film on the external surface (λ_c = 100 W/mK). Their theoretical and experimental work in Dalian, China, documented a 12% efficiency gain compared to a control copper-fin U-tube ETC and attributed this gain to augmented conductive contact between the manifold and glass.

Kabeel et al. [124] built a coaxial heat-pipe manifold of seven coaxial R22/R134a-charged tubes, which were inserted in evacuated tubes with filling ratios between 30% and 60%. The manifold, tested in Alexandria at air mass flow rates of up to 0.009 kg/s, demonstrated efficiency gains of up to 67% when optimally inclined at 20°, highlighting the potential of refrigerant selection and manifold design for transient operation. Abd-Elhady et al. [125] combined oil infusion and foamed copper inserts in the annulus between a 4 cm inner-diameter tube and its 5 cm outer-diameter shell, finding that the hybrid oil-foamed-metal configuration raised heat-pipe tip temperatures by 25% and efficiency by 55.6% (vs. 42.7% using oil alone), emphasizing how porous metal matrices may be employed to supplement base fluids to maximize conduction. Kumar et al. [126] investigated the possibilities of heating air in an ETC by placing an aluminium tube with fifteen tubes in different directions and using it to heat the air in Haryana, India. They discovered that the efficiency rose to 16% at a mass flow rate of 10.13 kg/h, and the maximum air temperature at the outflow was 72.7°C when a properly dimensioned inserted tube was used in arrayed systems, demonstrating the importance of dimensioning the inserted tube. According to Yang et al. [127], the insertion of special stainless steel or plastic tubes in the manifold header of a thirty-tube all-glass ETC can be used to heat forced water. By showing a simple retrofit that yields greater uniformity in the distribution of manifolds, the dynamic numerical model numerically demonstrated that the optimum tube diameter is 32 mm, with a range of 59.99 to 55.19% at water flows below 1.6 kg/s.

Aggarwal et al. [128] compared copper and aluminium fin materials in a 58 mm outer diameter, 1.8 m long heat-pipe ETC array with a tilt of 20-50°. During performance testing in Himachal Pradesh, India, at 5 L/h, copper fins achieved a maximum of 58.57%, compared with 51.50% for aluminium fins. The optimal tilt of 30° resulted in ~14% greater performance for copper, indicating the influence of material thermal conductivity and emissivity on collector performance. Zhang et al. [129] placed an aluminium heat shield below the absorber plate of a coaxial direct-flow ETC, and a 31.49% efficiency enhancement and a 50.80% decrease in heat-loss coefficient were reported with the shield in place compared to the unshielded design, reflecting the effectiveness of selective thermal shields at medium-temperature water heating. In Jowzi et al. [130], the problem of stagnation zones was solved by introducing a bypass tube with a diameter of 2 m and a length of 10 mm into a two-tube ETC manifold. Bypass was effective in their hybrid CFD/experimental study in Kermanshah, where it eradicated dead zones and provided a 25% increase in heat gain and an 11% increase in efficiency, illustrating thermal non-uniformities can be overcome by simply redirecting the flow. Tamuli et al. [131] numerically solved a flat absorber plate with inner and outer concentric pipes (6 mm and 12 mm diameter) in a coaxial open-type ETC of 6.4 m^2 aperture and attained modeled efficiency up to ~80% at 1000 W/m^2, which proves the promise of hybrid plate-pipe absorbers in northeastern Indian conditions. Using a nine-tube air heating ETC, Zaphar et al. [132] tested a one-ended stainless steel manifold with directional inner tubes and found, that, at an air flow of 15.14 kg/h and a tube diameter of 20 mm, DT was 62.5°C and efficiency was 32.9%, indicating an optimal design under mixed operating conditions. The thermal and exergy analysis of the triple-meshed helical coil revealed a higher Nu, lower exergy loss, and a relatively small pressure drop penalty, highlighting the importance of geometric alteration [133]. A turbulator using a wire coil for a helical tube suggested around 13% increase in heat transfer and around 10% increase in effectiveness due to enhanced internal convection [134], while a compact helical geometry showed up to a 12.42% increase in heat transfer coefficient and 12.77% increase in COP [135]. These indirect studies also suggested that turbulence-in-

ducing designs lower thermal resistance and enhance mixing. Introducing these design changes into ETCs would lead to better internal convection and thermal efficiency.

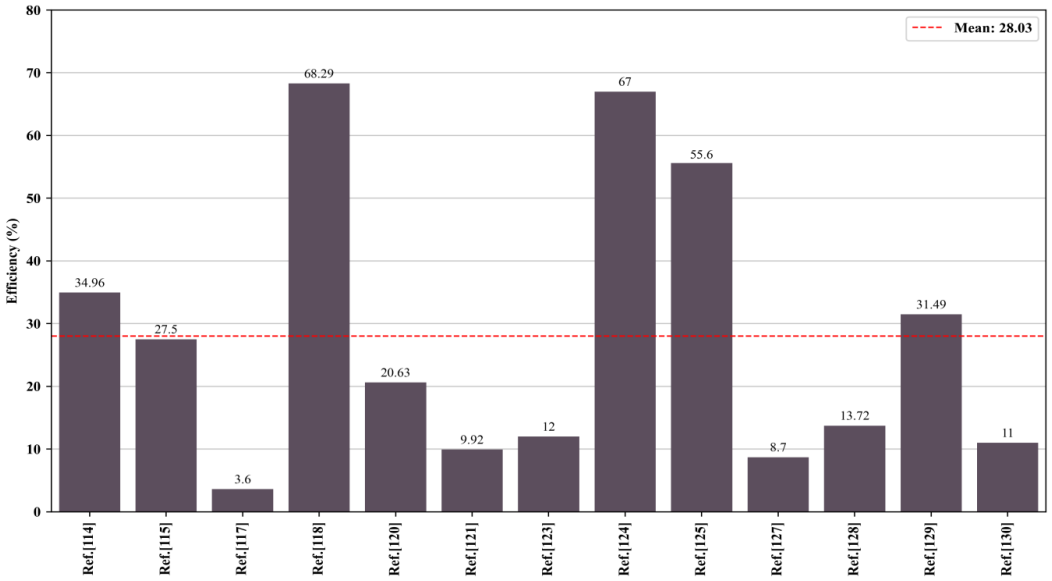

Figure 7. Efficiency enhancement using design alterations

Figure 7 illustrates the improvement in efficiency for the respective studies resulting from design alterations. Design modifications, such as helical coils, coaxial manifolds, and porous inserts, have significantly improved performance by optimising internal heat transfer and fluid flow. These advantages come at the expense of fluid-dynamic performance, i.e., increased pressure drop, as well as increased manufacturing complexity and material compatibility issues. Thus, optimum performance is highly sensitive to the particular coordination of insert geometry, flow, and thermal boundary conditions.

Table 4. ETCs featuring design innovations

Ref.	Alteration	Design details	Methodology highlights	Key performance parameters	Quantitative enhancement
Supankanok et al. [114]	Stainless-steel scrubbers	Void fraction ~2%; Weight ~109.7 g., Inserted in gap between evacuated tube (ID 0.047 m, OD 0.058 m, L 1.8 m) and copper heat pipe (OD 0.014 m), HTF: 10 mol% EG-water	Experimental & Mathematical modeling (Ladkrabang, Bangkok)	Heat pipe tip temp.. ETC efficiency, Overall heat transfer coefficient, Breakeven	Avg. HTF temp. in modified tube 160.32°C (vs. 138.71°C standard; ~22°C higher), Efficiency increased by 34.96%, UA increased 10-fold, Breakeven shorten (vs. standard) by ~ 12 months
Agade et al. [115]	WT and PWT insert	PWT: 6 mm equilateral triangles (6 PWT), 9 mm equilateral triangles (9 PWT), WT: Copper strip 0.3 mm thick, 16 mm wide, 1200 mm long, folded at 20 mm intervals, 60° angle, ETC: 8 tubes, 1.5 m length, 1.5 m^2 aperture area	Experimental; comparative analysis (Madhya Pradesh, India)	Hourly, Daily and Exergy efficiency	6 PWT: highest efficiencies-83.33% hourly, 49.36% daily energy and exergy gains, higher by 70.18%

Yao et al. [116]	Twist tape inserts	Twist tap: L_t = 1.7 m; W = 0.044 m; δ = 0.001 m; twist pitches P = 0.110 m (y = 2.5), P = 0.176 m (y = 4), Collector tube: D = 0.047 m; L = 1.8 m; Tank ID = 0.36 m; Tilt 45°	Numerical (CFD) for a single collector tube model	Nu, Heat transfer	Mean Nu (vs. normal): y = 2.5: -1.07%; y = 4.0: +9.29%, Inserts help heat transfer at high temp, not at low temp.
Kumar et al. [117]	LFPTT	Helical twist ratio (y/D) = 2, 2.5, 3 & Tape hole diameter ratio (d/D) = 0.0714, 0.107, 0.143	Analytical model	Effective thermal efficiency, Exergy efficiency, Airflow rates	Peak thermal efficiency 62.33% (at 400 kg/h; y/D = 2; d/D = 0.0714), Peak exergy efficiency 3.91%, Highest efficiency at lower airflow rates
Said et al. [118]	Helical tube (as a heat exchanger)	59 turns, total pipe length 5730 mm, OD 54 mm, Fitted on inner glass tube (dia. 58/54 mm, length 700 mm), Pipe dia. 7.94 mm	Experimental (indoor, solar simulator: 15 lamps, 1000 W/m^2); compared to heat pipe, U-tube, double U-tube, coaxial ETC	Thermal efficiency	Helical tube ETC: Thermal efficiency 69% (vs. 31% for heat pipe; 41-54% for other direct flow)
Kumar et al. [119]	Inserted baffles	Baffle length varied, Tube OD 57 mm; ID 48 mm & length 1800 mm	Experimental & Analytical; at different mass flow rates (Tamil Nadu, India)	Temp. rise, Thermal performance	Max temp. rise 42.8°C, Baffles enhance thermal efficiency; increased baffle length improves temp. rise & thermal efficiency at the cost of pumping power
Mukuna and Gryzagoridis [120]	Internal geometry inserts	No insert (NI); I-profile (II); V-profile (VI); Triangle (TI), Square (SI), Copper sheet 0.7 mm thick, HP: OD 8 mm, L 1720 mm, ETC tube: OD 58 mm, L 1800 mm, Fluids: acetone, ethanol, etc., distilled water	Experimental (indoor, solar simulator 700 W/m^2; tested in Durban, South Africa)	Efficiency	Dry mode: Efficiency 20.3% (NI) to 24.4% (SI) & Distilled water: η 53.3% (NI) to 64.3% (SI); square profile best
Singh and Vardhan [121]	Helical coiled inserts	ETC with co-axial pipes (dia. 20 mm): OD 58 mm; ID 47 mm; length 1800 mm, Helical coils: wire dia. 1.5 mm; coil dia. 47 mm; pitch ratio 1	Experimental; at different mass flow rates (Punjab, India)	Outlet temp., Thermal efficiency, Pressure loss	Max outlet temp. 112.6°C (at 0.003 kg/s), Max thermal efficiency 70.9% (vs. 64.5% at 0.015kg/s), ETC-HI outperformed simple ETC despite 2.45 times pressure drop; with no added cost
Singla et al. [122]	Rib roughening (half absorber tube)	Relative roughness pitch (P/e) = 6-12, Relative roughness height (e/D) = 0.071 (fixed), Heat input 1000 W/m^2	CFD analysis for different relative roughness pitches and mass flow rates	Nu, Friction factor (f), Thermo-hydraulic performance parameter	Nu increased by 1.88 times vs. smooth, f increased by 2.89 times vs. smooth, THPP = 1.36 (at R_e = 8000; P/e = 10)
Liang et al. [123]	Filled layer	Two-layered glass ETC (length 1450 mm; U-tube: dia. 8 mm & outer glass tube: dia. 47 mm, 1.2 mm thick) absorber film on outer surface of absorber tube (dia. 37 mm, 1.2 mm thick)	Theoretical & Experimental (Dalian, China)	Efficiency	Efficiency 12% higher than U-tube ETC with copper fin (when λ_c = 100 W/m K)
Kabeel et al. [124]	Modified coaxial heat pipes	7 coaxial heat pipes inside evacuated tubes: ID/OD 12.7/28.57 mm; length 1500 mm and manifold 1050 mm; Filling ratios 30-60% with R22/R134a	Experimental; at different air mass flow rates (Alexandria, Egypt)	Thermal efficiency	Max efficiency increased by 67% at 0.009 kg/s using heat pipes (compared to without) at the optimum tilt angle of 20°

Abd-Elhady et al. [125]	Foamed copper filled the gap between the heat pipe and the inner wall of the evacuated tube (with oil)	Evacuated tube: 1.5 m length; 5 cm OD; 4 cm ID, Oil volume: 1-1.6 L, Foamed copper porosity: 50%	Experimental; comparative analysis (Beni-Suef, Egypt)	Heat pipe temp.. Heating efficiency	Temp. Increase: 25% (with oil + foamed copper), Efficiency increase: 42.7% (with oil); 55.6% (with oil + foamed copper)
Kumar et al. [126]	Directional inner Al tubes	15 evacuated tubes: each 1.5 m long; OD 0.047 m; absorber tube 0.037 m, Manifold 1.16 m, Aluminium tube (varied length) dia.: 0.01 m	Experimental; varying air flow rates (Haryana, India)	ΔT, Efficiency	Max temp. rise: 72.7°C at 5.06 kg/h, Max efficiency: 16% at 10.13 kg/h (0.83 m Al tubes)
Yang et al. [127]	Inserted stainless steel/ plastic tube in manifold header	30 evacuated tubes (dia. 58 × 1800 mm); inserted tube dia. = 18-32 mm; manifold: 2550 × 1950 mm; water tank: 300 L	Dynamic numerical model, with experimental validation (Jiaxing, China)	Collector efficiency	Efficiency up from 55.19% to 59.99% (~5% gain); optimal inserted tube dia.: 32 mm; water mass flow <1.6 kg/s
Aggarwal et al. [128]	Fin material (Copper vs. Aluminium)	1800 mm length evacuated tubes, 58 mm OD, 45 mm ID; 10-litre tank; tilt angles: 20°, 30°, 40°, 50°	Experimental; comparison across inclination angles & flow rates (Himachal Pradesh, India)	Thermal efficiency	Max efficiency with copper: 58.57%; with aluminium: 51.50% at 5 L/h; Efficiency improved by ~14% with copper over aluminium
Zhang et al. [129]	Aluminium heat shield inserted below the absorber plate	Evacuated tube: 2000 mm long, OD 100 mm / ID 94 mm; absorber: 1915 mm × 92 mm (0.12 mm thick copper with TiNOx coating); coaxial flow conduit dia. 8 mm; 6 tubes per collector	Experimental; comparative study	Collection efficiency	Heat shield boosted efficiency by 31.49%
Jowzi et al. [130]	Addition of a bypass tube to eliminate the stagnant region	Evacuated tube-2 nos..: 1.8 m (OD/ID = 58/45 mm); absorber area: 0.242 m^2, Bypass tube: 2 m length; 10 mm dia. (optimum), 7 L tank, 45° tilt	Experimental & CFD (COMSOL) analysis (Kermanshah, Iran)	Average tank temp.., Useful heat gain, Efficiency	Efficiency up by 11%, Useful heat gain up by 25%, Tank average temp. up by 1.5°C vs. typical ETC
Tamuli et al. [131]	Co-axial pipe integration with a flat absorber plate	Absorber: TiNOx coated flat plate, Inner pipe: 6 mm outer, 5.3 mm inner diameter, Outer pipe: 12 mm outer, 10.4 mm inner diameter, Pipe length: 1750-1820 mm, Absorber plate: 1700 mm × 60 mm, thickness 0.2 mm, Aperture area: 6.4 m^2	Numerical (MATLAB) modeling (Assam, India)	Efficiency	Max efficiency: ~80% (At I = 1000 w/m^2)
Zaphar et al. [132]	One-ended stainless steel manifold with inner directional stainless steel tubes	9 evacuated tubes, each 1.5 m long, Stainless steel tube: 1.27 m long, dia. 10 & 20 mm, Outer/inner glass dia.: 47/37 mm, Manifold: 0.96 m long, CPVC pipe with 0.02 m dia.	Experimental; at different air mass flow rates (Uttar Pradesh, India)	ΔT, Efficiency	Max ΔT 62.5°C, T_{out} 90.5°C at 4.58 kg/h, Max efficiency 32.9% at 15.14 kg/h (20 mm tube dia.)

3.5. Hybrid methods

The quest for ever-increasing performance has driven engineers to explore hybrid enhancement approaches, whereby two or more individual techniques are combined to leverage synergistic opportunities. Hybrid methods aim to overcome the shortcomings of single-aspect enhancements, providing greater benefits in thermal performance, energy delivery, and overall system performance. Several studies employing hybrid methods to enhance the performance of ETC have been reviewed, as shown in Table 5. Algarni et al. [136] investigated a nano-enhanced PCM(Ne-PCM),combining paraffin with 0.33 wt% Cu nanoparticles, within a U-pipe ETC under the arid conditions of Abha, Saudi Arabia, and reported a striking 32% improvement in thermal efficiency compared to conventional paraffin PCM. Building on this, Alshukri et al. [137] combined micro-ZnO and nano-CuO particles at 5 wt% with paraffin wax in a heat-pipe ETC subject to varied flow rates in Najaf, Iraq. Their empirical results demonstrated that collector efficiency increased to 88.5% at an optimal flow rate of 3 L/h (i.e., 97.68% over the baseline heat-pipe ETC), underscoring the synergistic effect of dual-scale particulates on heat transfer augmentation. Felinski and Sekret [138] mixed technical-grade paraffin PCM and a CPC in a heat-pipe ETC and demonstrated a mean charging efficiency enhancement of 5% and peak charging efficiency enhancements of up to 9% compared to non-concentrated designs. Sadeghi et al. [139] also extended hybrid setups by using a low-concentration Cu_2O/water nanofluid(0.01-0.08 %vol)with a parabolic concentrator on a passive circulation ETC; experimental and numerical studies conducted at Kermanshah, Iran, showed that the energy efficiency increased from 68%(pure water and no reflector)to 78% while using a 0.08 %vol nanofluid and concentrator and increased exergy efficiency from 14 to 26.7%, economic payback time of only 3 years. Essa et al. [140] incorporated helical fins into a heat-pipe ETC with paraffin wax PCM in Zagazig, Egypt, and combined experimental measurement with theoretical modeling for a range of flow rates to demonstrate a daily efficiency increase of 13.6-15% over standard fin geometry with the added benefit of enhanced temperature uniformity within the PCM matrix. Agade [141] investigated a binary eutectic PCM composed of palmitic and stearic acids embedded with a copper wavy tape insert in a U-tube ETC in Madhya Pradesh, India, and recorded a maximal hourly efficiency of 71.75%, an average daily efficiency of 45.92%, an average exergy efficiency of 6.11%, and a notable 35.5% reduction in CO_2 emissions relative to baseline systems. Senobar et al. [142] experimented with copper metal foam embedded with paraffin PCM in a heat-pipe ETC and reported outlet water temperatures up to 77% higher than inlet temperatures, and 2-3 times higher rate of PCM melting compared to pure paraffin, thereby demonstrating the potential of porous metal matrices in accelerating thermal charge-discharge rates.

Deshmukh et al. [143] introduced twisted tape inserts(twist ratio H/D = 5)within a U-tube ETC and circulated a TiN/water nanofluid at volume fractions up to 0.1%; tests in Maharashtra, India, across multiple flow rates revealed enhancements of 23.96% in thermal conductivity, a staggering 378.87% increase in the Nu number, a 475.37% rise in convective HTC, and an overall solar thermal efficiency reaching 80.47% at 1.25 L/min and 0.1 %vol. Sobhansarbandi et al. [144] developed a multilayer carbon-nanotube(CNT)coating on the absorber coupled with paraffin(octadecane)PCM in a heat-pipe ETC in Texas, USA, achieving up to 98% solar spectral absorption(600-1100 nm)while leveraging the PCM to buffer thermal output for quasi-steady delivery. Manirathnam et al. [145] combined paraffin PCM with SCi & CuO nanoparticles(1 mass%)in an all-glass ETC with thermosyphonic flow in Tamil Nadu, India, reporting energy efficiencies of 33.8% without PCM, 38.3% with pure PCM, and 41.7% with nano-composite PCM, alongside exergy efficiencies of 1.78%, 2.18%, and 3.23%, respectively, and a 22.53% increase in PCM thermal conductivity. Kumar and Mylsamy [146] tested paraffin PCM with 0.5%, 1.0%, and 2.0% mass fractions of nano-CeO_2 incorporated in a water-in-glass ETC under thermosyphon mode of operation in Tamil Nadu; maximum energy and exergy efficiencies of 79.2% and 5.1%, respectively, were achieved at 1.0% CeO_2, which justified the fine tuning of nanoparticle concentration for balanced heat storage and release. Embracing multi-functional hybrids, Yang et al. [147] performed a numerical evaluation of a novel PV/T-PCM unit, designated FETC-PV-PCM; they reported overall power output rising from 33.89 W to 38.42 W, a 13% efficiency increase, with an additional 3.37% performance gain at 4 wt% MWCNT nanofluid and further output boosts via reduced PCM melting points. Elbrashy et al. [148] integrated paraffin wax PCM containing 0.2 wt% CuO nanoparticles into an ETC coupled with a solar air heater in Kafrelsheikh, Egypt, and by varying air flow rates demonstrated a maximal thermal efficiency of 62.66% with nano-enhanced PCM vs. 37.34% without at 0.05 kg/s, achieving a peak useful energy gain of 2735 W at 0.006 kg/s.

Tabarhoseini and Sheikholeslami [149] performed numerical analysis of a thermosyphonic flow ETC with longitudinal absorber fins and water-based Cu/MWCNT nanofluid at 1%, 3%, and 5% volume fractions, realizing peak thermal efficiency of 65.21% at complete nanoparticles loading; at this condition, useful heat gain was 116.11 kJ and optical efficiency was enhanced to 67.61%, showing synergetic gains due to fins and multi-scale nanoparticles. Ghaderian et al. [150] examined an internal spiral coil heat exchanger immersed in a U-tube ETC and circulated CuO/distilled water nanofluids at 0.03-0.06 %vol in Johor, Malaysia; experimental data revealed thermal efficiencies up to 51.4% at 0.06% loading and 41.9% at 0.03%, with average outlet temperatures elevated by nearly 14% over pure water benchmarks at 60 L/h. In Tamil Nadu, Kumar and Mylsamy [151] compared paraffin PCM enhanced with 1.0 mass% SiO_2 nanoparticles in an all-glass ETC under thermosyphonic flow, reporting energy efficiencies of 58.74% (no PCM), 69.62% (pure PCM), and 74.79% (NCPCM); exergy efficiencies of 19.6%, 22.0%, and 24.6% for those configurations, respectively; and a 22.78% increase in PCM thermal conductivity due to SiO_2 nanoparticles.

Abokersh et al. [152] merged paraffin wax PCM (ALEX WAX 600) with aluminium extended-fins in a U-tube ETC equipped with a forced recirculation solar water heating system in Cairo, Egypt, and employed both experimental trials and TRNSYS-based long-term simulations to demonstrate a maximum annual thermal efficiency of 85.7% for finned configurations (vs. 71.8% unfinned and 40.5% for the baseline forced solar water heating system (FSWHS)), real-time efficiencies of 33% (finned), 26% (unfinned), and 20% (FSWHS), and a 47.7% increase in energy discharge for the finned PCM module. Olfian et al. [153] numerically assessed a U-tube ETC with a spirally corrugated U-shaped tube immersed in paraffin PCM in Babol, Iran, and found that corrugation increased collector efficiency by 21.55% relative to a smooth-tube counterpart with the same PCM. Kabeel et al. [154] experimented with hybrid PCM composed of paraffin wax and graphite (0-5 wt%) in a modified U-tube ETC featuring cylindrical parabolic concentrators in Gharbia, Egypt; by varying feed water rates, daily thermal efficiencies escalated from a baseline of 44.4-51.3% (without PCM) to 75.2-88.2% with 5 wt% graphite, and useful heat gain peaked at 71.1% under the same conditions. Naghavi et al. [155] presented a theoretical model of a heat-pipe ETC with PCM housed in the manifold and an internal finned heat exchanger. Their simulations in Kuala Lumpur, Malaysia, indicated that above a flow rate of 55 L/h, the hybrid system consistently outperformed conventional heat-pipe collectors in thermal efficiency. Although the FPCs were the primary target, these findings have significant implications for improving the performance of ETC. Sheikholeslami et al. [156] conducted experimental research on twisted-tape inserts with nanofluids. They observed that the transformation of the nanoparticles from spherical to blade-like increased heat transfer by approximately 12.12% and thermal efficiency by approximately 17.26%. They stated that a rise in the inlet velocity resulted in a remarkable increase in Nu of approximately 264.12%. They also observed an increase in pumping power, which resulted in a 9.06% reduction in total efficiency, demonstrating the trade-off when ETC is used. In another study, Sheikholeslami et al. [157] numerically investigated a new turbulator using an MWCNT-Al2O3 hybrid nanofluid, employing the RNG k-ϵ model. They proposed Nu increases of up to 75.22% and reductions in friction factors of about 12.43%. They also noted geometry-based changes in the friction factor and Nu of approximately -6.57% and -66.89%, respectively. This shows that judiciously designed turbulator shapes can lead to enhanced convective heat transfer and mixing. Hence, suitable attention should be paid to the pressure drop, manufacturability, cost and scalability.

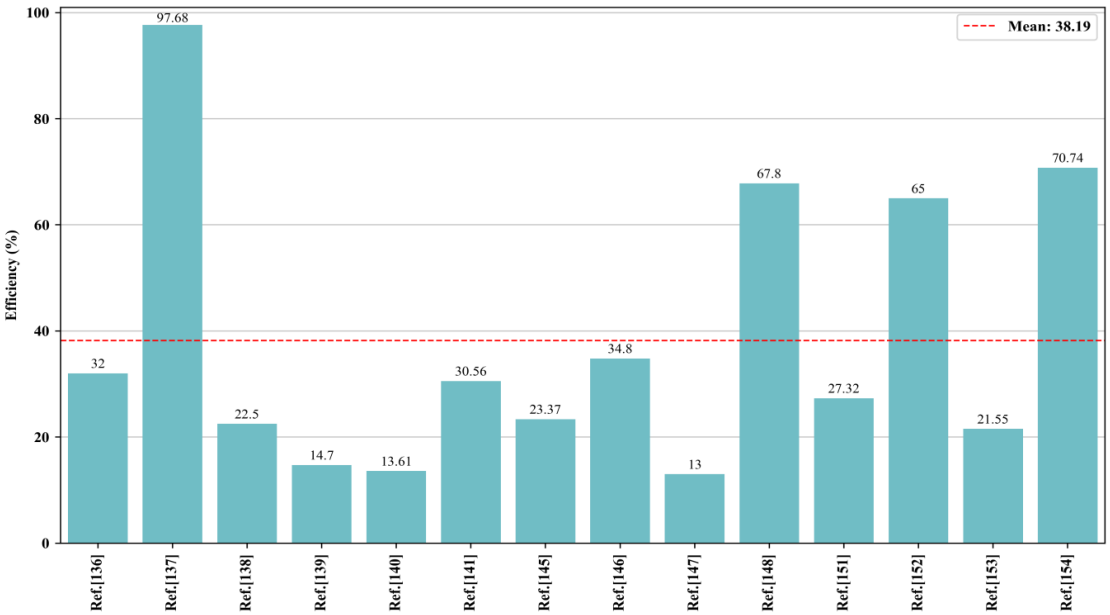

Figure 8. Efficiency enhancement using hybrid methods

The efficiency gains in the studies reviewed above are shown in Figure 8. The nano-enhanced PCM, extended heat-transfer surface and optical concentrator show considerable improvements in hybrid methods. These studies show that the multifaceted integration can increase the thermal efficiencies of ETCs to a higher level, increase the useful daily energy output and offer possible ways to reduce the payback period to as low as three years.

Table 5. ETCs utilizing hybrid approaches

Ref.	Hybrid techniques	Methodology highlights	Key performance parameters	Quantitative enhancement
Algarni et al. [136]	Nano-enhanced PCM (Ne-PCM: paraffin + 0.33 wt% Cu nanoparticles)	Experimental (Abha, Saudi Arabia)	Efficiency	32% efficiency enhancement
Alshukri et al. [137]	Micro-ZnO and nano-CuO particles with Paraffin wax (5 wt%)	Experimental; varied flow rates (Najaf, Iraq)	Efficiency	Up to 88.5% efficiency (at 3 L/h flow rate)
Felinski and Sekret [138]	PCM (technical-grade paraffin) and CPC	Experimental	Avg. charging efficiency, Max. charging efficiency	Avg. charging efficiency up by 5%, Max. charging efficiency up by 9%
Sadeghi et al. [139]	Nanofluid (Cu_2O/DI water; 0.01-0.08 %vol) and Parabolic concentrator	Experimental & Numerical (Kermanshah, Iran)	Energy & Exergy efficiency, Payback	Energy efficiency improved from 68% (pure water; w/o reflector) to 78% (with 0.08 %vol nanofluid and PC). Exergy efficiency increased from 14% to 26.7%, with a Payback of 3 years.
Essa et al. [140]	PCM (paraffin wax) and Helical fins	Experimental & Theoretical; varied flow rates (Zagazig, Egypt)	Daily efficiency	Helical fins: Daily efficiency by 13.6-15% > conventional fins (with PCM); better temp. homogeneity
Agade [141]	Binary eutectic PCM (palmitic + stearic acid) and Copper wavy tape	Experimental (Madhya Pradesh, India)	Hourly efficiency, Daily avg. efficiency, Avg. exergy efficiency, CO2 mitigation	PCM+WT: Max hourly efficiency 71.75%, Avg. daily efficiency 45.92%, Avg. exergy efficiency 6.11%, CO2 reduction up by 35.5% (highest of all configs.)
Senobar et al. [142]	PCM (paraffin wax) and Copper metal foam	Experimental	Outlet water temp.	Max outlet water temp. 77% higher than input and 2-3 times faster melting rate (vs. pure PCM)
Deshmukh et al. [143]	Nanofluid (TiN/water; 0.0-0.1 %vol) and Twisted tape inserts (H/D = 5)	Experimental; varied flow rates (Maharashtra, India)	Thermal performance	Improved thermal conductivity by 23.96%, Nu number by 378.87%, HTC by 475.37% and Solar efficiency to 80.47% at 0.1 %vol & 1.25 L/min
Sobhansarbandi et al. [144]	Carbon Nanotube (CNT) multilayer absorber and Paraffin (octadecane)	Experimental (Texas, USA)	Solar absorption, Heat storage and output	CNT coating: Max 98% solar absorption (600-1100 nm), PCM for storage & constant output
Manirathnam et al. [145]	Paraffin wax with SCi & CuO nanoparticles (1.0 mass%)	Experimental (Tamil Nadu, India)	Energy & Exergy efficiency, Thermal conductivity	Energy efficiency: 33.8% (no PCM); 38.3% (PCM); 41.7% (NCPCM), Exergy efficiency: 1.78%; 2.18%; 3.23%, Thermal conductivity up by 22.53%
Kumar and Mylsamy [146]	Paraffin PCM with Nano-CeO2 at 0.5%, 1.0%, and 2.0% mass fractions	Experimental (Tamil Nadu, India)	Energy & Exergy efficiency	Max energy efficiency: 79.2%, Exergy efficiency: 5.1%; (at 1.0% CeO2)

Yang et al. [147]	PV/T-PCM hybrid unit	Numerical	Overall performance	Overall power output: 38.42 W (FETC-PV-PCM) vs. 33.89 W (ETC-PCM), Efficiency up by 13%, Nanofluid (4 wt% MWCNT) up performance by 3.37% and reduced PCM melting point-up output by 0.4%
Elbrashy et al. [148]	Paraffin wax PCM with CuO nanoparticles (0.2 wt%)	Experimental; varied air flow rates (Kafrelsheikh, Egypt)	Efficiency, Energy gain	Max efficiency: 62.66% with NE-PCM vs. 37.34% without at 0.05 kg/s, Max useful energy gain: 2735 W (with NE-PCM at 0.006 kg/s)
Tabarhoseini and Sheikholeslami [149]	Longitudinal fins within absorber with Nanofluid (water-based Cu/MWCNT in 1, 3, 5% volume fractions	Numerical	Thermal efficiency, Heat gain, Optical efficiency	Thermal efficiency up to 65.21% with longitudinal fins, 5% MWCNT in finned case: useful heat gain of 116.11 kJ & Optical efficiency 67.61% (compared to unfinned and finned with Cu nanofluid)
Ghaderian et al. [150]	Internal spiral coil with CuO/distilled water nanofluid (0.03-0.06 %vol).	Experimental; varied flow rates (Johor, Malaysia)	Efficiency, Average temp. output	Efficiency increased to 51.4% (0.06% CuO) and 41.9% (0.03% CuO) at 60 L/h, Average temp. output increased by almost 14% (at 0.03-0.06% CuO)
Kumar and Mylsamy [151]	Paraffin PCM with 1.0 mass% SiO2 nanoparticles	Experimental (Tamil Nadu, India)	Energy & Exergy efficiency, Thermal conductivity	Energy efficiency: 58.74% (w/o PCM); 69.62% (PCM); 74.79% (NCPCM), Exergy efficiency: 19.6% (w/o PCM); 22.0% (PCM); 24.6% (NCPCM), Thermal conductivity of paraffin increased by 22.78% with silica nanoparticles
Abokersh et al. [152]	Paraffin wax PCM (ALEX WAX 600) integrated with Al-Fin (extended surfaces)	Experimental & Regression-based long-term simulation via TRNSYS (Cairo, Egypt)	Efficiency, Energy discharge	Max. annual efficiency: 85.7% (finned); 71.8% (un-finned) vs. 40.5% (FSWHS) & Real-time efficiency: 33% (finned); 26% (un-finned); 20% (FSWHS), Energy discharge up by 47.7% (finned) and 35.8% (unfinned) under clear sky
Olfian et al. [153]	PCM (paraffin wax) with U-shaped spirally corrugated tube	Numerical (Babol, Iran)	Collector efficiency	Corrugated tube increased the collector efficiency by 21.55% compared to the smooth tube with PCM.
Kabeel et al. [154]	Hybrid PCM (paraffin wax + graphite, 0-5 wt%) with Cylindrical parabolic concentrators	Experimental; varied feed water rates (Gharbia, Egypt)	Daily thermal efficiency, Heat gain	Daily efficiency up from 44.4-51.3% (no PCM) to 75.2-88.2%, Useful heat gain up to 71.1% (at 5% graphite)
Naghavi et al. [155]	PCM (paraffin wax in manifold) with a Finned internal heat exchanger	Theoretical modeling (Kuala Lumpur, Malaysia)	Thermal efficiency	Higher thermal efficiency than conventional heat pipe ETC at flow rate > 55 L/h

3.6. Comparative analysis

The average efficiency improvement for the ETCs varies across techniques, as shown in Figure 9: hybrid methods lead with 38.19% (range 13.61 to 97.68%), followed by design alterations at 28.03% (3.6 to 68.29%), PCMs at 24.29% (5.56 to 55.7%), nanofluids at 22.84% (1.85 to 71.84%), and reflectors/concentrators at 20.40% (2.8 to 33%). Range bars indicate variability, with performance being highly dependent on test conditions and protocols.

The selection of thermal performance enhancement techniques for the ETCs requires balancing cost, complexity, O&M, and durability: the following comparative analysis table supports informed, application-specific decisions.

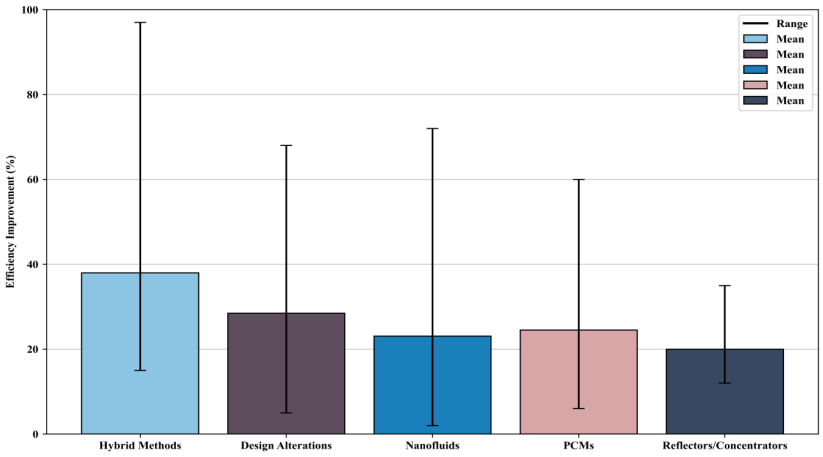

Figure 9. Efficiency gains across enhancement techniques

Table 6. Comparative summary of enhancement techniques

Technique reviewed [Ref.]	Avg. thermal efficiency gain (in %)	Reported range (in %)	Relative capital cost	Installation & O&M complexity	Main limitations/ durability challenge	Best-suited application/ primary advantage
Nanofluids [16-61]	22.84	1.85-71.84	Medium-High	High (preparation & monitoring)	Colloidal instability, abrasion/corrosion, increased viscosity/ pressure drop, potential optical absorption and environmental/toxicity issues	Medium-temperature processes requiring high heat-transfer rates; raise conductivity and convective HTC
Phase change materials [62-90]	24.29	5.56-55.7	Medium	Medium (integration, added weight)	Low thermal conductivity, volume change/leakage, supercooling and cycling degradation	Applications needing stable/extended heat output (e.g., overnight storage); smooths diurnal fluctuations
Reflectors/ Concentrators [91-113]	20.40	2.8-33	Low (static) - High (tracking)	Low (static) - High (tracking)	Optical soiling/ degradation, alignment/ structural issues, increased thermal stress at high concentration	Yield boost in low-irradiance regions (static); raises outlet temperature for mid-temp. applications (concentrating)
Design alterations [114-135]	28.03	3.6-68.29	Low (retrofit inserts) - Medium (integrated)	Low (retrofit) - Medium (increased pumping)	Increased pressure drop/ pumping work, erosion/ material compatibility, and manufacturing complexity for integrated solutions	Broad performance improvement for new or existing direct-flow systems; favourable near-term trade-off
Hybrid methods (combinations) [136-157]	38.19	13.61-97.68	High	High (multi-system integration & control)	Compound reliability risks (component interactions), complex thermal/mechanical integration, and higher capex	High-performance or high-temperature applications where maximizing output justifies cost/complexity.

The techno-economic evaluation of enhanced ETCs suggests balancing performance and yields against capital costs, operation and maintenance complexity, and long-term durability. Low-temperature applications (below 80°C, such as domestic hot water) benefit most from cost-effective design improvements and reflectors, including the addition of a copper fin and a diffuse flat reflector. In contrast, medium-temperature applications (ranging from 80°C to 150°C, such as industrial process heat and solar cooling) are bet-

ter suited to investment in hybrid systems, such as nano-enhanced PCMs with extended heat-transfer surfaces and optical concentrators. Although nanofluids and PCMs present greater technical complexity, design modifications offer appealing short-term solutions. However, over the long term, hybrid systems, despite their higher costs, provide the best value when integration and economic factors are favourable, making them promising candidates for high-performance solar thermal applications.

4. Societal value

The studies reviewed show that the application of a number of techniques to enhance the thermal performance of solar evacuated-tube collectors has a social value. The paper enables transitions that optimise thermal efficiency, increase the period of heat supply and minimise greenhouse gas emissions. It allows the decarbonisation of heat supply and enhances access to high-quality thermal services for industrial and domestic users. Social benefits include lower fuel poverty, lower air pollution and improved health, more jobs in clean energy supply chains, and greater resilience through localised thermal supply. The transfer of technical performance to policy and research agendas and the effective integration of social and academic knowledge for sustainable and equitable use of high-efficiency collectors is ensured.

5. Conclusion

This review consolidates experimental, numerical and field studies of thermal performance improvement for solar evacuated tube collectors, revealing technique-specific trade-offs. The literature reviewed reports a broad range of thermal efficiency improvements: nanofluids and nanoparticle-enhanced heat transfer fluids from 1.85% to 71.84% (average ≈22.84%), phase change materials from 5.56% to 55.7% (average ≈24.29%), reflectors/concentrators from 2.8% to 33% (average ≈20.40%), and geometry or internal-design changes from 3.6% to 68.29% (average ≈28.03%). The combination of complementary measures that address different aspects of the system yield the greatest range and mean system-level improvement (13.61% to 97.68%, average ≈38.19%) but also the most complexity and risk. While numerous studies report impressive instantaneous and daily improvements, there are unaddressed limitations: nanofluids are plagued by instability, abrasion, and absorption (which reduces collector transmittance); phase change materials are limited by low intrinsic thermal conductivity, volume change, and cycling degradation; reflectors need maintenance to maintain reflectivity and alignment; and many internal design inserts increase pressure drop and pumping energy. Crucially, percentage gains are dependent on the starting system design, test protocol and operating conditions, making it difficult to compare results across studies and to undertake meta-analysis. As such, the most solid conclusion is conditional: specific measures can significantly improve the thermal performance of evacuated tube collectors (with average improvements in the 20-40% range for each major technique); but gains depend on holistic design choices, ageing under realistic cycling, and trade-offs between thermal gains and parasitic or life-cycle costs. Consistent metrics, long-term cycling tests and techno-economic analysis are critical to translate laboratory-scale gains to real-world conditions and guide deployment.

6. Future work

In light of the identified gaps, future research needs to be an interdisciplinary, integrated approach that combines laboratory innovation with rigorous field testing and techno-economic analysis. First, nanofluid research needs to prioritise long-term stability under thermal- and shear-cycling conditions representative of the intended use, to perform mechanistic studies of agglomeration and abrasion, to report zeta potential and rheological data, and to choose or encapsulate environmentally safe nanoparticles to avoid toxicity and disposal problems. Secondly, PCM incorporation includes the use of conductivity-enhancing features (finned tubes, graphite foams, nanoparticle doping), stable PCM encapsulation to prevent leakage and volume change, and the cycle-life testing under realistic transient heat loads to determine degradation and its effect on system efficiency. Third, concentrator and reflector designs must be evaluated for dirt tolerance, anti-fouling coating effectiveness, misalignment tolerance and strength under wind and dusty environments. Also, life-cycle reflectivity and cleaning loads need to be monitored along with instantaneous optical gains. Fourth, design innovations and insertion technologies need to be optimised for coupled thermo-hydraulic performance, via multi-objective optimisation that explicitly balances thermal gain versus pumping penalty and cost. Fifth, hybrid systems need system-level demonstration tests that integrate storage, optical concentration and enhanced fluids to verify laboratory gains (hybrid averages ≈38.19%) in real-world climates and to discover new failure modes. In all cases, researchers should adopt standardized testing protocols (insolation and test inlet and outlet conditions, uncertainty analysis), open data, and interoperable simulation models to enable meta-analysis. Sixth, policy-focused research on life-cycle analysis, levelized heat cost, supply-chain material availability, and training needs will ensure laboratory efficiency gains are equitably and replicably translated into decarbonization of industrial and distributed energy applications. International testing standards set by industry consortia and standards bodies will facilitate commercialisation and enable claims.

Copyright and permission statement

Nomenclature

COP28	28th Conference of the Parties
ETC	Evacuated Tube Collector
FPC	Flat Plate Collector
PCM	Phase Change Material
HTF	Heat Transfer Fluid

HTC	Heat Transfer Coefficient
DHW	Domestic Hot Water
PTC	Parabolic Trough Collector
CPC	Compound Parabolic Concentrator
DFR	Diffuse Flat Reflector
CFD	Computational Fluid Dynamics
HP-ETC	Heat-Pipe Evacuated Tube Collector
GAHP	Gravity-Assisted Heat Pipe
SETAH	Solar Evacuated Tube Air Heater
ETC-HI	Evacuated Tube Collector Helical Inserts
CVFEM	Control Volume-based Finite Element Method
LFPTT	Loose-Fit Perforated Twisted Tape
PWT	Perforated Wavy Tape
WT	Wavy Tape
FSWHS	Forced Recirculation Solar Water Heating System
MSS3(CaO)	Modified Solar Stills with Calcium Oxide
UV	Ultraviolet
mV	Millivolts
DSC	Differential Scanning Calorimetry
TGA	Thermogravimetric Analysis
FTIR	Fourier-Transform Infrared Spectroscopy
RNG	Renormalization Group theory
PV/T	Photovoltaic/Thermal
ORC	Organic Rankine Cycle
G	Global Solar Irradiance
CR	Concentration Ratio
COP	Coefficient of Performance
Nu	Nusselt Number
f	Friction Factor
FR	Heat Removal Factor
PEM	Polymer Electrolyte Membrane
THPP	Thermo-Hydraulic Performance Parameter
O&M	Operations and Maintenance
Re	Reynolds Number
P/e	Relative Roughness Pitch
e/D	Relative Roughness Height
y/D	Helical Twist Ratio
d/D	Tape-Hole Diameter Ratio
P	Pitch
D, L	Tube Diameter and Length (Generic Dimensions)
ΔT	Temperature Difference
UA	Overall Heat Transfer Coefficient X Area

Chemical formulas & symbols

H_2O	Water (Base Fluid)
CO_2	Carbon Dioxide
SO_2	Sulfur Dioxide
Al_2O_3	Aluminium Oxide
TiO_2	Titanium Dioxide
SiO_2	Silicon Dioxide
CuO	Copper Oxide
ZnO	Zinc Oxide
CeO_2	Cerium Oxide
WO_3	Tungsten Trioxide
MgO	Magnesium Oxide
Al	Aluminium
Ag	Silver
SWCNT	Single-Walled Carbon Nanotube
MWCNT	Multi-Walled Carbon Nanotube
GNP	Graphene Nanoplatelets
EG	Ethylene Glycol
Fe_3O4	Ferrosoferric Oxide
Cu_2O	Copper Oxide
$Ba(OH)_2{\cdot}8H_2O$	Barium Hydroxide Octahydrate
$BaCO_3$	Barium Carbonate
TiNOx	Titanium Nitride Oxide
pH	Potential of Hydrogen
PVP	Polyvinylpyrrolidone
SDBS	Sodium Dodecylbenzenesulfonate
Paraffin wax	Paraffin Formulations (e.g. RT-40, Technical Grade, ALEX WAX 600), Stearic Acid ($C_{18}H_{36}O_2$), Palmitic Acid ($C_{16}H_{32}O_2$)

Greek symbols

η	Efficiency
ΔT	Temperature Difference
λ	Thermal Conductivity
α	Solar Absorptance
ε	Thermal Emissivity
k	Turbulent Kinetic Energy
ϵ	Dissipation Rate

Subscripts

in	Inlet
out	Outlet
m	Mean or Reference
en	Energy
ex	Exergy

References

[1] Mevada, D., Panchal, H., ElDinBastawissi, H. A., Elkelawy, M., Sadashivuni, K., Ponnamma, D., Thakar, N., & Sharshir, S. W. (2019). Applications of evacuated tubes collector to harness the solar energy: a review. International Journal of Ambient Energy, 43(1),344–361. https://doi.org/10.1080/01430750.2019.1636886

[2] Kumar, A. R., & Ramakrishnan, M.(2022).A scoping review on recent advancements in domestic applications of solar thermal systems. Journal of Thermal Engineering, 8(3),426–444. https://doi.org/10.18186/thermal.1117446

[3] IEA(2024),COP28 Tripling Renewable Capacity Pledge, IEA, Paris https://www.iea.org/reports/cop28-tripling-renewable-capacity-pledge, Licence: CC BY 4.0

[4] Kumar, R., Dhapekar, N. K., Tiwari, R., Rao, Y. A., Narain, R. S., Yadav, A. S., & Sharma, A. (2023). Prospects of renewable energy scenario in India. In Engergy systems in electrical engineering (pp. 15–31). https://doi.org/10.1007/978-981-99-6116-0_2

[5] Sultan, K. F., Anead, H. S., & Jabber, S. A.(2020).The nano fluid effect on the plethora of thermal efficiency in evacuated tube solar collector. IOP Conference Series Materials Science and Engineering, 978(1),012029. https://doi.org/10.1088/1757-899x/978/1/012029

[6] Chopra, K., Tyagi, V., Pandey, A., & Sari, A.(2018).Global advancement on experimental and thermal analysis of evacuated tube collector with and without heat pipe systems and possible applications. Applied Energy, 228, 351–389. https://doi.org/10.1016/j.apenergy.2018.06.067

[7] Sabiha, M., Saidur, R., Mekhilef, S., & Mahian, O.(2015). Progress and latest developments of evacuated tube solar collectors. Renewable and Sustainable Energy Reviews, 51, 1038–1054. https://doi.org/10.1016/j.rser.2015.07.016

[8] C. Porras-Prieto, C. J., Lizcano, J., García, J. L., & Mazarrón, F. R.(2018).Energy saving in an ETC solar system to produce high temperature water. Energies, 11(4),840. https://doi.org/10.3390/en11040840

[9] Aggarwal, S., Kumar, R., Kumar, S., Bhatnagar, M., & Kumar, P.(2021).Computational fluid dynamics based analysis for optimization of various thermal enhancement techniques used in evacuated tubes solar collectors: A review. Materials Today Proceedings, 46, 8700–8707. https://doi.org/10.1016/j.matpr.2021.04.021

[10] Deshmukh, K., & Karmare, S.(2021).A review on convective heat augmentation techniques in solar thermal collector using nanofluid. Journal of Thermal Engineering, 7(5),1257–1266. https://doi.org/10.18186/thermal.978064

[11] Ali, B. H., Gilani, S., & Al-Kayiem, H. H.(2013).Investigation of evacuated tube collector performance at high temperature mode using TRNSYS simulation model. Applied Mechanics and Materials, 465–466, 155–160. https://doi.org/10.4028/www.scientific.net/amm.465-466.155

[12] Ali, S. H., Eidan, A. A., & Sahlani, A. A.(2021).Study the Effect of Phase Change Material on the Performance of Evacuated Tube Heat Pipe Solar Collector under Iraqi Climatic Conditions. IOP Conference Series Materials Science and Engineering, 1094(1),012009. https://doi.org/10.1088/1757-899x/1094/1/012009

[13] Kumar, A., Said, Z., & Bellos, E.(2020).An up-to-date review on evacuated tube solar collectors. Journal of Thermal Analysis and Calorimetry, 145(6),2873–2889. https://doi.org/10.1007/s10973-020-09953-9

[14] Kumar, N., Yadav, A. S., Sudarshan, N., Kumar, S., Shankar, R., Kumar, R., Alam, T., Sharma, A., Siddiqui, M. I. H., & Dobrotă, D. (2025). Location and panel based performance evaluation of solar photovoltaic system for remote Indian deserts. Case Studies in Thermal Engineering, 74, 106795. https://doi.org/10.1016/j.csite.2025.106795

[15] HajiBeiGy, M. T., Walvekar, R., & Cv, A.(2020).MATHEMATICAL MODELLING, SIMULATION ANALYSIS OF a PHOTOVOLTAIC THERMAL SYSTEM. Journal of Thermal Engineering, 7(1),291–306. https://doi.org/10.18186/thermal.850645

[16] Al-Gebory, L.(2021).OPTICAL AND RADIATIVE PROPERTIES OF INDIVIDUAL AND HYBRID NANOSUSPENSIONS: THE EFFECTS OF SIMILAR AND DISSIMILAR PARTICLE AGGLOMERATES ON THERMAL RADIATION. Journal of Thermal Engineering, 7(2),174–186. https://doi.org/10.18186/thermal.871304

[17] Sabiha, M., Saidur, R., Hassani, S., Said, Z., & Mekhilef, S.(2015).Energy performance of an evacuated tube solar collector using single walled carbon nanotubes nanofluids. Energy Conversion and Management, 105, 1377–1388. https://doi.org/10.1016/j.enconman.2015.09.009

[18] Iranmanesh, S., Ong, H. C., Ang, B. C., Sadeghinezhad, E., Esmaeilzadeh, A., & Mehrali, M.(2017).Thermal performance enhancement of an evacuated tube solar collector using graphene nanoplatelets nanofluid. Journal of Cleaner Production, 162, 121–129. https://doi.org/10.1016/j.jclepro.2017.05.175

[19] Iranmanesh, S., Silakhori, M., Naghavi, M. S., Ang, B. C., Ong, H. C., & Esmaeilzadeh, A.(2021).Using graphene nanoplatelets nanofluid in a Closed-Loop evacuated tube Solar Collector—Energy and Exergy Analysis. Journal of Composites Science, 5(10),277. https://doi.org/10.3390/jcs5100277

[20] Daghigh, R., & Zandi, P.(2018).Improving the performance of heat pipe embedded evacuated tube collector with nanofluids and auxiliary gas system. Renewable Energy, 134, 888–901. https://doi.org/10.1016/j.renene.2018.11.090

[21] Eidan, A. A., AlSahlani, A., Ahmed, A. Q., Al-Fahham, M., & Jalil, J. M.(2018).Improving the performance of heat pipe-evacuated tube solar collector experimentally by using Al2O3 and CuO/acetone nanofluids. Solar Energy, 173, 780–788. https://doi.org/10.1016/j.solener.2018.08.013

[22] López-Núñez, O. A., Lara, F., González-Angeles, A., Cardenas-Robles, A., Ramírez-Minguela, J., & Alfaro-Ayala, J. A.(2024).Assessment of thermohydraulic performance and entropy generation in an evacuated tube solar collector employing pure water and nanofluids as working fluids. Heliyon, 10(8),e29309. https://doi.org/10.1016/j.heliyon.2024.e29309

[23] Khudair, N. Y., & Husain, A. K.(2024).Investigation the Performance of an Evacuated Tube Solar Collector Filled with MWCNT/ Water Nanofluid Under the Climate Conditions of Al-Hilla(Iraq).Journal of Petroleum Research and Studies, 14(3),135–154. https://doi.org/10.52716/jprs.v14i3.865

[24] Al-Abayechi, N. Y., Alaiwi, N. Y., & Al-Khafaji, N. Z.(2024). Exploration of key approaches to enhance evacuated tube solar collector efficiency. Journal of Advanced Research in Numerical Heat Transfer, 19(1),1–14. https://doi.org/10.37934/arnht.19.1.114

[25] Surve, S. S.(2023).Enhancing Thermal Performance of Evacuated Tube Solar Collector using Novel Graphene Oxide Nanofluid. ASM Science Journal, 18, 1–14. https://doi.org/10.32802/asmscj.2023.1477

[26] Mahendran, M., Lee, G., Sharma, K., & Shahrani, A.(2012). Performance of Evacuated Tube Solar Collector using Water-Based Titanium Oxide Nanofluid. JOURNAL OF MECHANICAL ENGINEERING AND SCIENCES, 3, 301–310. https://doi.org/10.15282/jmes.3.2012.6.0028

[27] Ghaderian, J., & Sidik, N. a. C.(2017).An experimental investigation on the effect of Al2O3/distilled water nanofluid on the energy efficiency of evacuated tube solar collector. International Journal of Heat and Mass Transfer, 108, 972–987. https://doi.org/10.1016/j.ijheatmasstransfer.2016.12.101

[28] Sharafeldin, M., & Gróf, G.(2018).Evacuated tube solar collector performance using CeO2/water nanofluid. Journal of Cleaner Production, 185, 347–356. https://doi.org/10.1016/j.jclepro.2018.03.054

[29] Yurddaş, A.(2020).Optimization and thermal performance of evacuated tube solar collector with various nanofluids. International Journal of Heat and Mass Transfer, 152, 119496. https://doi.org/10.1016/j.ijheatmasstransfer.2020.119496

[30] Hosseini, S. M. S., & Dehaj, M. S.(2020).Assessment of TiO2 water-based nanofluids with two distinct morphologies in a U type evacuated tube solar collector. Applied Thermal Engineering, 182, 116086. https://doi.org/10.1016/j.applthermaleng.2020.116086

[31] Shahi, M., Mahmoudi, A. H., & Talebi, F.(2010).Numerical simulation of steady natural convection heat transfer in a 3-dimensional single-ended tube subjected to a nanofluid. International Communications in Heat and Mass Transfer, 37(10),1535–1545. https://doi.org/10.1016/j.icheatmasstransfer.2010.08.005

[32] Lu, L., Liu, Z., & Xiao, H.(2011).Thermal performance of an open thermosyphon using nanofluids for high-temperature evacuated tubular solar collectors. Solar Energy, 85(2),379–387. https://doi.org/10.1016/j.solener.2010.11.008

[33] Tong, Y., Kim, J., & Cho, H.(2015).Effects of thermal performance of enclosed-type evacuated U-tube solar collector with multi-walled carbon nanotube/water nanofluid. Renewable Energy, 83, 463–473. https://doi.org/10.1016/j.renene.2015.04.042

[34] Kaya, H., Arslan, K., & Eltugral, N.(2018b).Experimental investigation of thermal performance of an evacuated U-Tube solar collector with ZnO/Etylene glycol-pure water nanofluids. Renewable Energy, 122, 329–338. https://doi.org/10.1016/j.renene.2018.01.115

[35] Kim, H., Ham, J., Park, C., & Cho, H.(2015).Theoretical investigation of the efficiency of a U-tube solar collector using various nanofluids. Energy, 94, 497–507. https://doi.org/10.1016/j.energy.2015.11.021

[36] Mahbubul, I., Khan, M. M. A., Ibrahim, N. I., Ali, H. M., Al-Sulaiman, F. A., & Saidur, R.(2018).Carbon nanotube nanofluid in enhancing the efficiency of evacuated tube solar collector. Renewable Energy, 121, 36–44. https://doi.org/10.1016/j.renene.2018.01.006

[37] Ozsoy, A., & Corumlu, V.(2018).Thermal performance of a thermosyphon heat pipe evacuated tube solar collector using silver-water nanofluid for commercial applications. Renewable Energy, 122, 26–34. https://doi.org/10.1016/j.renene.2018.01.031

[38] Dehaj, M. S., & Mohiabadi, M. Z.(2018).Experimental investigation of heat pipe solar collector using MgO nanofluids. Solar Energy Materials and Solar Cells, 191, 91–99. https://doi.org/10.1016/j.solmat.2018.10.025

[39] Kaya, H., & Arslan, K.(2018).Numerical investigation of efficiency and economic analysis of an evacuated U-tube solar collector with different nanofluids. Heat and Mass Transfer, 55(3),581–593. https://doi.org/10.1007/s00231-018-2442-z

[40] Sharafeldin, M., & Gróf, G.(2018b).Efficiency of evacuated tube solar collector using WO3/Water nanofluid. Renewable Energy, 134, 453–460. https://doi.org/10.1016/j.renene.2018.11.010

[41] Yan, S., Wang, F., Shi, Z., & Tian, R.(2017).Heat transfer property of SiO 2 /water nanofluid flow inside solar collector vacuum tubes. Applied Thermal Engineering, 118, 385–391. https://doi.org/10.1016/j.applthermaleng.2017.02.108

[42] M. Jamil, M. M., Sidik, N. C., & Yazid, M. M.(2016).Thermal performance of thermosyphon evacuated tube solar collector using TiO2/water nanofluid. Journal of Advanced Research in Fluid Mechanics and Thermal Sciences, 20(1),12-29

[43] Gan, Y. Y., Ong, H. C., Ling, T. C., Zulkifli, N., Wang, C., & Yang, Y.(2018).Thermal conductivity optimization and entropy generation analysis of titanium dioxide nanofluid in evacuated tube solar collector. Applied Thermal Engineering, 145, 155–164. https://doi.org/10.1016/j.applthermaleng.2018.09.012

[44] Saxena, G., & Gaur, M. K.(2020).Energy, exergy and economic analysis of evacuated tube solar water heating system integrated with heat exchanger. Materials Today Proceedings, 28, 2452–2462. https://doi.org/10.1016/j.matpr.2020.04.793

[45] Elshazly, E., Abdel-Rehim, A. A., & El-Mahallawi, I. (2022). Thermal performance enhancement of evacuated tube solar collector using MWCNT, Al2O3, and hybrid MWCNT/Al2O3nanofluids. International Journal of Thermofluids, 17, 100260. https://doi.org/10.1016/j.ijft.2022.100260

[46] Sathish, T., Saravanan, R., Arunachalam, S. J., Giri, J., Al-lehaibi, M., & Lalvani, J. I. J.(2025).Enhancement of hydrogen production using an integrated evacuated tube solar collector and PEM electrolyzer with AL2O3 and SIO2 hybrid nanofluids. Engineering Reports, 7(2).https://doi.org/10.1002/eng2.13103

[47] Henein, S. M., & Abdel-Rehim, A. A.(2022b).The performance response of a heat pipe evacuated tube solar collector using MgO/MWCNT hybrid nanofluid as a working fluid. Case Studies in Thermal Engineering, 33, 101957. https://doi.org/10.1016/j.csite.2022.101957

[48] Shahini, N., Karami, M., & Behabadi, M. a. A.(2024).Numerical investigation of direct absorption evacuated tube solar collector using alumina nanofluid. Journal of Thermal Engineering, 562–571. https://doi.org/10.14744/thermal.0000825

[49] Gerdroodbary, M. B. (2019). Application of neural network on heat transfer enhancement of magnetohydrodynamic nanofluid. Heat Transfer-Asian Research, 49(1),197–212. https://doi.org/10.1002/htj.21606

[50] Man, Y., & Gerdroodbary, M. B. (2024). INFLUENCE OF LORENTZ FORCES ON FORCED CONVECTION OF NANOFLUID IN a POROUS ENCLOSURE. Journal of Porous Media, 27(8),15–25. https://doi.org/10.1615/jpormedia.2024025325

[51] Gerdroodbary, M. B., Jafaryar, M., Sheikholeslami, M., & Amini, Y. (2023). The efficacy of magnetic force on thermal performance of ferrofluid in a screw tube. Case Studies in Thermal Engineering, 49, 103187. https://doi.org/10.1016/j.csite.2023.103187

[52] Manh, T. D., Abazari, A. M., Gerdroodbary, M. B., Nam, N. D., Moradi, R., & Babazadeh, H. (2020). Computational simulation of variable magnetic force on heat characteristics of backward-facing step flow. Journal of Thermal Analysis and Calorimetry, 144(4),1585–1596. https://doi.org/10.1007/s10973-020-09608-9

[53] Ouabouch, O., Kriraa, M., & Lamsaadi, M. (2021). Stability, thermophsical properties of nanofluids, and applications in solar collectors: A review. AIMS Materials Science, 8(4),659–684. https://doi.org/10.3934/matersci.2021040

[54] Moghaieb, H. S., Amendola, V., Khalil, S., Chakrabarti, S., Maguire, P., & Mariotti, D. (2023). Nanofluids for Direct-Absorption Solar Collectors—DASCs: A review on recent progress and future Perspectives. Nanomaterials, 13(7),1232. https://doi.org/10.3390/nano13071232

[55] Bocanegra, J. A., Marchitto, A., & Misale, M. (2024). Nanofluids in solar collectors: a comprehensive review focused on its sedimentation. Clean Technologies and Environmental Policy. https://doi.org/10.1007/s10098-024-02964-2

[56] Yu, W., & Xie, H. (2011). A review on nanofluids: preparation, stability mechanisms, and applications. Journal of Nanomaterials, 2012(1).https://doi.org/10.1155/2012/435873

[57] Wole-Osho, I., Okonkwo, E. C., Abbasoglu, S., & Kavaz, D. (2020). Nanofluids in solar thermal Collectors: Review and limitations. International Journal of Thermophysics, 41(11). https://doi.org/10.1007/s10765-020-02737-1

[58] Manimaran, M., Norizan, M. N., Kassim, M. H. M., Adam, M. R., Abdullah, N., & Norrrahim, M. N. F. (2025). Critical review on the stability and thermal conductivity of water-based hybrid nanofluids for heat transfer applications. RSC Advances, 15(18),14088–14125. https://doi.org/10.1039/d5ra00844a

[59] Zainon, S., & Azmi, W. (2021). Recent Progress on Stability and Thermo-Physical Properties of Mono and Hybrid towards Green Nanofluids. Micromachines, 12(2),176. https://doi.org/10.3390/mi12020176

[60] Mishra, P. C., Mukherjee, S., Nayak, S. K., & Panda, A. (2014). A brief review on viscosity of nanofluids. International Nano Letters., 4(4),109–120. https://doi.org/10.1007/s40089-014-0126-3

[61] Kalsi, S., Kumar, S., Kumar, A., Alam, T., Sharma, A., & Yadav, A. S. (2025). A review on hybrid nanofluids for heat transfer: advancements, synthesis, challenges and applications. Deleted Journal, 7(7).https://doi.org/10.1007/s42452-025-07141-8

[62] Kumar, R., Rao, Y. A., Yadav, A. S., Balu, A., Panda, B. P., Joshi, M., Taneja, S., & Sharma, A. (2022). Application of phase change material in thermal energy storage systems. Materials Today Proceedings, 63, 798–804. https://doi.org/10.1016/j.matpr.2022.06.152

[63] Papadimitratos, A., Sobhansarbandi, S., Pozdin, V., Zakhidov, A., & Hassanipour, F.(2016).Evacuated tube solar collectors integrated with phase change materials. Solar Energy, 129, 10–19. https://doi.org/10.1016/j.solener.2015.12.040

[64] Chopra, K., Pathak, A. K., Tyagi, V., Pandey, A., Anand, S., & Sari, A.(2019).Thermal performance of phase change material integrated heat pipe evacuated tube solar collector system: An experimental assessment. Energy Conversion and Management, 203, 112205. https://doi.org/10.1016/j.enconman.2019.112205

[65] Feliński, P., & Sekret, R.(2017).Effect of PCM application inside an evacuated tube collector on the thermal performance of a domestic hot water system. Energy and Buildings, 152, 558–567. https://doi.org/10.1016/j.enbuild.2017.07.065

[66] Abokersh, M. H., El-Morsi, M., Sharaf, O., & Abdelrahman, W.(2017).An experimental evaluation of direct flow evacuated tube solar collector integrated with phase change material. Energy, 139, 1111–1125. https://doi.org/10.1016/j.energy.2017.08.034

[67] Xue, H. S.(2015).Experimental investigation of a domestic solar water heater with solar collector coupled phase-change energy storage. Renewable Energy, 86, 257–261. https://doi.org/10.1016/j.renene.2015.08.017

[68] Feng, L., Liu, J., Lu, H., Chen, Y., & Wu, S.(2022).A parametric study on the efficiency of a solar evacuated tube collector using phase change materials: A transient simulation. Renewable Energy, 199, 745–758. https://doi.org/10.1016/j.renene.2022.09.029

[69] Li, Y., Liang, X., Song, W., Li, T., Wang, D., & Liu, Y.(2022). Optimization and thermal performance of U-type evacuated tube solar collector filled with phase change material. Energy Reports, 8, 6126–6138. https://doi.org/10.1016/j.egyr.2022.04.054

[70] Said, S., Mellouli, S., Alqahtani, T., Algarni, S., Ajjel, R., Alshammari, B. M., & Kolsi, L.(2024).Performance enhancement of evacuated U-tube solar collector integrated with phase change material. Case Studies in Thermal Engineering, 61, 104948. https://doi.org/10.1016/j.csite.2024.104948

[71] Pathak, S. K., Tyagi, V. V., Chopra, K., Pandey, A. K., Sari, A., & Abdulateef, A. M.(2023).Energetic, Exergetic, and heat transfer assessment of PCM-Integrated Heat-Pipe-Based ETSC for clear and cloudy weather conditions. Sustainability, 15(12),9780. https://doi.org/10.3390/su15129780

[72] Essa, M. A., Mostafa, N. H., & Ibrahim, M. M. (2018). An experimental investigation of the phase change process effects on the system performance for the evacuated tube solar collectors integrated with PCMs. Energy Conversion and Management, 177, 1–10. https://doi.org/10.1016/j.enconman.2018.09.045

[73] Bazri, S., Badruddin, I. A., Naghavi, M. S., Seng, O. K., & Wongwises, S.(2019).An analytical and comparative study of the charging and discharging processes in a latent heat thermal storage tank for solar water heater system. Solar Energy, 185, 424–438. https://doi.org/10.1016/j.solener.2019.04.046

[74] Naghavi, Ong, K., Badruddin, I., Mehrali, M., Silakhori, M., & Metselaar, H.(2015).Theoretical model of an evacuated tube heat pipe solar collector integrated with phase change material. Energy, 91, 911–924. https://doi.org/10.1016/j.energy.2015.08.100

[75] Chopra, K., Tyagi, V., Pathak, A. K., Pandey, A., & Sari, A.(2019).Experimental performance evaluation of a novel designed phase change material integrated manifold heat pipe evacuated tube solar collector system. Energy Conversion and Management, 198, 111896. https://doi.org/10.1016/j.enconman.2019.111896

[76] Fang, W., Riffat, S., & Wu, Y.(2017).Experimental investigation of evacuated heat pipe solar collector efficiency using phase-change fluid. International Journal of Low-Carbon Technologies, 12(4),392–399. https://doi.org/10.1093/ijlct/ctx010

[77] Wu, W., Dai, S., Liu, Z., Dou, Y., Hua, J., Li, M., Wang, X., & Wang, X.(2018).Experimental study on the performance of a novel solar water heating system with and without PCM. Solar Energy, 171, 604–612. https://doi.org/10.1016/j.solener.2018.07.005

[78] Pawar, V. R., & Sobhansarbandi, S.(2020).CFD modeling of a thermal energy storage based heat pipe evacuated tube solar collector. Journal of Energy Storage, 30, 101528. https://doi.org/10.1016/j.est.2020.101528

[79] Alshukri, M. J., Eidan, A. A., & Najim, S. I.(2021).Thermal performance of heat pipe evacuated tube solar collector integrated with different types of phase change materials at various location. Renewable Energy, 171, 635–646. https://doi.org/10.1016/j.renene.2021.02.143

[80] Li, B., & Zhai, X.(2017).Experimental investigation and theoretical analysis on a mid-temperature solar collector/storage system with composite PCM. Applied Thermal Engineering, 124, 34–43. https://doi.org/10.1016/j.applthermaleng.2017.06.002

[81] Bai, Y., He, X., Liu, Y., Duan, J., Wang, Y., & Han, X. (2018). Experimental investigation of a solar thermal storage heater assembled with finned heat pipe and collective vacuum tubes. Energy Conversion and Management, 166, 463–473. https://doi.org/10.1016/j.enconman.2018.04.034

[82] Khan, Y., Tevatia, A., Apparao, D., Singh, N., & Mishra, S.(2024).Experimental investigation to evaluate thermal performance of a solar cooker with evacuated tube solar collector using different heat transfer fluids. Journal of Thermal Engineering, 1335–1346. https://doi.org/10.14744/thermal.0000873

[83] Raj, G., Prabhansu, Kumar, R., Chandra, P., & Saurabh, S. (2019). Experimental study of solar still augmented with low-cost energy absorbing and releasing materials. Energy Sources Part a Recovery Utilization and Environmental Effects, 42(1),56–65. https://doi.org/10.1080/15567036.2019.1587054

[84] Abdalla, F., Tuohy, P., Evans, D., & Blackwell, P. (2018). A review of integrated phase change materials for evacuated tube solar collector system. International Conference on Energy Research. https://strathprints.strath.ac.uk/66957/

[85] Rathod, M. K., & Banerjee, J. (2012). Thermal stability of phase change materials used in latent heat energy storage systems: A review. Renewable and Sustainable Energy Reviews, 18, 246–258. https://doi.org/10.1016/j.rser.2012.10.022

[86] Sharma, A., Tyagi, V., Chen, C., & Buddhi, D. (2008). Review on thermal energy storage with phase change materials and applications. Renewable and Sustainable Energy Reviews, 13(2),318–345. https://doi.org/10.1016/j.rser.2007.10.005

[87] Singh, S. K., Verma, S. K., Kumar, R., Sharma, A., Singh, R., & Tiwari, N. (2022). Experimental analysis of latent heat thermal energy storage system using encapsulated multiple phase-change materials. Proceedings of the Institution of Mechanical Engineers Part E Journal of Process Mechanical Engineering, 238(1),124–133. https://doi.org/10.1177/09544089221110983

[88] Duttaluru, G., Ansu, A. K., Sharma, A., & Sharma, R. K. (2022). Study of eutectic organic phase change materials with enhanced thermal properties. Materials Today Proceedings, 63, 553–558. https://doi.org/10.1016/j.matpr.2022.03.706

[89] Singh, S., Verma, S., Kumar, R., Gupta, G., Pati, P. R., & Sharma, A. (2022). Thermal performance enhancement of CUO-Paraffin Nano-Enhanced phase change material. International Journal of Vehicle Structures and Systems, 14(3). https://doi.org/10.4273/ijvss.14.3.26

[90] Mohan, M., Manjunath, V., Mehdi, S. M. Z., Soni, S. K., Dewangan, S. K., Lee, H., Awasthi, A., Sharma, V. K., Sharma, A., Song, E., Lee, N., Heo, J., Lee, K., & Ahn, B. (2025). Phonon-photon synergy in phase change materials through

nano-engineered carbon materials for multifunctional applications. Energy Storage Materials, 104142. https://doi.org/10.1016/j.ensm.2025.104142

[91] Schumann, J., Schiebler, B., & Giovannetti, F.(2021).Performance Evaluation of an Evacuated Tube Collector with a Low-Cost Diffuse Reflector. Energies, 14(24),8209. https://doi.org/10.3390/en14248209

[92] Altaher, N. a. A., Abd-Elhady, N. M. S., El-Sheikh, N. M. N., & Ahmed, N. S. A.(2022).The Effect of Using Secondary Reflectors on the Thermal Performance of Solar Collectors with Evacuated Tubes. Journal of Advanced Research in Fluid Mechanics and Thermal Sciences, 99(2),187–196. https://doi.org/10.37934/arfmts.99.2.187196

[93] Chai, S., Yao, J., Liang, J., Chiang, Y., Zhao, Y., Chen, S., & Dai, Y.(2021).Heat transfer analysis and thermal performance investigation on an evacuated tube solar collector with inner concentrating by reflective coating. Solar Energy, 220, 175–186. https://doi.org/10.1016/j.solener.2021.03.048

[94] Abo-Elfadl, S., Hassan, H., & El-Dosoky, M.(2020).Energy and exergy assessment of integrating reflectors on thermal energy storage of evacuated tube solar collector-heat pipe system. Solar Energy, 209, 470–484. https://doi.org/10.1016/j.solener.2020.09.009

[95] Pourbafrani, M., Ghadamian, H., Aminy, M., Moghadasi, M., Mardani, M., Akrami, M., ... & Sadr, S. M. K.(2024).Improving the Energy Performance of an Evacuated Tube Solar Collector Water Heater Using Compound Parabolic Concentrator: an Experimental Study. Journal of Renewable Energy and Environment, 11(2),58-66

[96] Sunkarwar, O. P., Naik, B. K., & Dasore, A.(2025).Experimental and Numerical Study of Parallel Flow Evacuated U-Tube Solar Collector with Parabolic Reflector: Impact of Particulate Matter. Journal of Solar Energy Engineering, 1–29. https://doi.org/10.1115/1.4067664

[97] Morrison, G., Budihardjo, I., & Behnia, M.(2004).Measurement and simulation of flow rate in a water-in-glass evacuated tube solar water heater. Solar Energy, 78(2),257–267. https://doi.org/10.1016/j.solener.2004.09.005

[98] Chen, F., Xia, E., & Bie, Y. (2019). Comparative investigation on photo-thermal performance of both compound parabolic concentrator and ordinary all-glass evacuated tube absorbers: An incorporated experimental and theoretical study. Solar Energy, 184, 539–552. https://doi.org/10.1016/j.solener.2019.04.036

[99] Milani, D., & Abbas, A.(2015).Multiscale modeling and performance analysis of evacuated tube collectors for solar water heaters using diffuse flat reflector. Renewable Energy, 86, 360–374. https://doi.org/10.1016/j.renene.2015.08.013

[100] Budihardjo, I., Morrison, G. L., & Behnia, M.(2007).Natural circulation flow through water-in-glass evacuated tube solar collectors. Solar Energy, 81(12),1460–1472. https://doi.org/10.1016/j.solener.2007.03.002

[101] Selvakumar, P., Somasundaram, P., & Thangavel, P.(2014b). Performance study on evacuated tube solar collector using therminol D-12 as heat transfer fluid coupled with parabolic trough. Energy Conversion and Management, 85, 505–510. https://doi.org/10.1016/j.enconman.2014.05.069

[102] Wang, J., Yin, Z., Qi, J., Ma, G., & Liu, X.(2015).Medium-temperature Solar Collectors with All-glass Solar Evacuated Tubes. Energy Procedia, 70, 126–129. https://doi.org/10.1016/j.egypro.2015.02.107

[103] Avargani, V. M., Rahimi, A., & Divband, M.(2020).Coupled optical and thermal analyses of a new type of solar water heaters using parabolic trough reflectors. Sustainable Energy Technologies and Assessments, 40, 100780. https://doi.org/10.1016/j.seta.2020.100780

[104] Naik, B. K., Premnath, S., & Muthukumar, P.(2021).Performance comparison of evacuated U-tube solar collector integrated parabolic reflector with conventional evacuated U-tube solar collector. Sadhana, 46(3).https://doi.org/10.1007/s12046-021-01656-7

[105] Dinesh, S., Ravi, S., Kumar, P. M., Subbiah, R., Karthick, A., Saravanakumar, P., & Pranav, R. A.(2021).Study on an ETC solar water heater using flat and wavy diffuse reflectors. Materials Today Proceedings, 47, 5228–5232. https://doi.org/10.1016/j.matpr.2021.05.561

[106] Ma, G., Yin, Z., Liu, X., Qi, J., & Dai, Y.(2020).Developments of CPC solar evacuated glass tube collector with a novel selective coating. Solar Energy, 220, 1120–1129. https://doi.org/10.1016/j.solener.2020.08.052

[107] Zambolin, E., & Del Col, D.(2010).Experimental analysis of thermal performance of flat plate and evacuated tube solar collectors in stationary standard and daily conditions. Solar Energy, 84(8),1382–1396. https://doi.org/10.1016/j.solener.2010.04.020

[108] Li, X., Dai, Y., Li, Y., & Wang, R.(2013).Comparative study on two novel intermediate temperature CPC solar collectors with the U-shape evacuated tubular absorber. Solar Energy, 93, 220–234. https://doi.org/10.1016/j.solener.2013.04.002

[109] Fathabadi, H.(2020).Impact of utilizing reflector, single-axis and two-axis sun trackers on the performance of an evacuated tube solar collector. International Journal of Green Energy, 17(12),742–755. https://doi.org/10.1080/15435075.2020.1798766

[110] De Paula Ribeiro Teles, M., Ismail, K. A., & Arabkoohsar, A.(2019).A new version of a low concentration evacuated tube solar collector: Optical and thermal investigation. Solar Energy, 180, 324–339. https://doi.org/10.1016/j.solener.2019.01.039

[111] T.N. Saadoon, N.F. Farman, and F.I. Mustafa, "Thermal efficiency Optimization of the evacuated tube Solar Water heater system by using mirror flat reflector," International Renewable Energy Congress(IREC),pp. 1–5, Oct. 2020, doi: 10.1109/IREC48820.2020.9310380

[112] Nkwetta, D. N., Smyth, M., Zacharopoulos, A., & Hyde, T.(2011).Optical evaluation and analysis of an internal low-concentrated evacuated tube heat pipe solar collector for powering solar air-conditioning systems. Renewable Energy, 39(1),65–70. https://doi.org/10.1016/j.renene.2011.06.043

[113] Jiang, C., Yu, L., Yang, S., Li, K., Wang, J., Lund, P. D., & Zhang, Y. (2020). A Review of the Compound Parabolic Concentrator (CPC) with a Tubular Absorber. Energies, 13(3),695. https://doi.org/10.3390/en13030695

[114] Supankanok, R., Sriwong, S., Ponpo, P., Wu, W., Chandra-Ambhorn, W., & Anantpinijwatna, A.(2021).Modification of a Solar Thermal Collector to Promote Heat Transfer inside an Evacuated Tube Solar Thermal Absorber. Applied Sciences, 11(9),4100. https://doi.org/10.3390/app11094100

[115] Agade, P. K., Agrawal, R., & Dubey, N.(2025).Augmenting the performance of evacuated tube solar water heater using perforated wavy tape. Solar Energy and Sustainable Development, 14(1),258–278. https://doi.org/10.51646/jsesd.v14i1.264

[116] Yao, K., Li, T., Tao, H., Wei, J., & Feng, K.(2015).Performance Evaluation of All-glass Evacuated Tube Solar Water Heater with Twist Tape Inserts Using CFD. Energy Procedia, 70, 332–339. https://doi.org/10.1016/j.egypro.2015.02.131

[117] Kumar, A. V., Arjunan, T., Seenivasan, D., Venkatramanan, R., Vijayan, S., & Matheswaran, M.(2021).Influence of twisted tape inserts on energy and exergy performance of an evacuated Tube-based solar air collector. Solar Energy, 225, 892–904. https://doi.org/10.1016/j.solener.2021.07.074

[118] Said, S., Mellouli, S., Alqahtani, T., Algarni, S., Ajjel, R., Ghachem, K., & Kolsi, L. (2023). An Experimental Comparison of the Performance of Various Evacuated Tube Solar Collector Designs TRANSLATE with x English Arabic Hebrew Polish Bulgarian Hindi Portuguese Catalan Hmong Daw Romanian Chinese Simplified Hungarian Russian Chinese Traditional Indonesian Slovak . . .. Sustainability, 15(6),5533. https://doi.org/10.3390/su15065533

[119] Kumar, A. V., Arjunan, T., Seenivasan, D., Venkatramanan, R., & Vijayan, S.(2021).Thermal performance of an evacuated tube solar collector with inserted baffles for air heating applications. Solar Energy, 215, 131–143. https://doi.org/10.1016/j.solener.2020.12.037

[120] Mukuna, J. G., & Gryzagoridis, J.(2020).The effect of different working fluids and internal geometries on the efficiency of evacuated tube heat pipe solar collectors. Journal of Energy in Southern Africa, 31(4),16–25. https://doi.org/10.17159/2413-3051/2020/v31i4a8480

[121] Singh, I., & Vardhan, S.(2020).Experimental investigation of an evacuated tube collector solar air heater with helical inserts. Renewable Energy, 163, 1963–1972. https://doi.org/10.1016/j.renene.2020.10.114

[122] Singla, M., Hans, V. S., & Singh, S.(2021).CFD analysis of rib roughened solar evacuated tube collector for air heating. Renewable Energy, 183, 78–89. https://doi.org/10.1016/j.renene.2021.10.055

[123] Liang, R., Ma, L., Zhang, J., & Zhao, D.(2011).Theoretical and experimental investigation of the filled-type evacuated tube solar collector with U tube. Solar Energy, 85(9),1735–1744. https://doi.org/10.1016/j.solener.2011.04.012

[124] Kabeel, A., Dawood, M. M. K., & Shehata, A. I. (2017). Augmentation of thermal efficiency of the glass evacuated solar tube collector with coaxial heat pipe with different refrigerants and filling ratio. Energy Conversion and Management, 138, 286–298. https://doi.org/10.1016/j.enconman.2017.01.048

[125] Abd-Elhady, Nasreldin, M., & Elsheikh, M.(2017).Improving the performance of evacuated tube heat pipe collectors using oil and foamed metals. Ain Shams Engineering Journal, 9(4),2683–2689. https://doi.org/10.1016/j.asej.2017.10.001

[126] Kumar, A., Kumar, S., & Yadav, A.(2014).Thermal performance analysis of evacuated tubes solar air collector in Indian climate conditions. International Journal of Ambient Energy, 37(2),162–171. https://doi.org/10.1080/01430750.2014.915884

[127] Yang, J., Jiang, Q., Hou, J., & Luo, C.(2015).A Study on Thermal Performance of a Novel All-Glass Evacuated Tube Solar Collector Manifold Header with an Inserted Tube. International Journal of Photoenergy, 2015, 1–7. https://doi.org/10.1155/2015/409517

[128] Aggarwal, S., Kumar, R., Kumar, S., & Singh, T.(2024).Impact of fin material properties and the inclination angle on the thermal efficiency of evacuated tube solar water heater: An experimental study. Journal of King Saud University - Science, 36(5),103186. https://doi.org/10.1016/j.jksus.2024.103186

[129] Zhang, X., You, S., Ge, H., Gao, Y., Xu, W., Wang, M., He, T., & Zheng, X.(2014).Thermal performance of direct-flow coaxial evacuated-tube solar collectors with and without a heat shield. Energy Conversion and Management, 84, 80–87. https://doi.org/10.1016/j.enconman.2014.04.014

[130] Jowzi, M., Veysi, F., & Sadeghi, G.(2019).Experimental and numerical investigations on the thermal performance of a modified evacuated tube solar collector: Effect of the bypass tube. Solar Energy, 183, 725–737. https://doi.org/10.1016/j.solener.2019.03.063

[131] Tamuli, B. R., Saikia, S. S., Nath, S., & Bhanja, D.(2019). Thermal performance analysis of a co-axial evacuated tube collector with single and two-phase flow consideration under North-eastern India climatic condition. Solar Energy, 196, 107–124. https://doi.org/10.1016/j.solener.2019.11.097

[132] Zaphar, S., M, N. C., & Verma, G.(2023).Thermal Analysis of an Evacuated Tube Solar Collector using a One-end Stainless Steel Manifold for Air Heating Applications under Diverse Operational Conditions. Evergreen, 10(2),897–911. https://doi.org/10.5109/6792885

[133] Kumar, R., & Chandra, P. (2019). Thermal analysis, pressure drop and exergy loss of energy efficient shell, and triple meshed helical coil tube heat exchanger. Energy Sources Part a Recovery Utilization and Environmental Effects, 42(8),1026–1039. https://doi.org/10.1080/15567036.2019.1602213

[134] Kumar, R., & Chandra, P.(2019).Thermal analysis of compact shell and wire coil-inserted helical coil tube heat exchanger. International Journal of Ambient Energy, 43(1),1068–1073. https://doi.org/10.1080/01430750.2019.1684992

[135] Kumar, R., Prabhansu, & Chandra, P.(2017).An experimental investigation of natural convection heat transfer over outer surface of vertical helical coil condenser. Journal of Engg. Research, 5(3),162–173

[136] Algarni, S., Mellouli, S., Alqahtani, T., Almutairi, K., Khan, A., & Anqi, A.(2020).Experimental investigation of an evacuated tube solar collector incorporating nano-enhanced PCM as a thermal booster. Applied Thermal Engineering, 180, 115831. https://doi.org/10.1016/j.applthermaleng.2020.115831

[137] Alshukri, M. J., Eidan, A. A., & Najim, S. I.(2021b).The influence of integrated Micro-ZnO and Nano-CuO particles/paraffin wax as a thermal booster on the performance of heat pipe evacuated solar tube collector. Journal of Energy Storage, 37, 102506. https://doi.org/10.1016/j.est.2021.102506

[138] Feliński, P., & Sekret, R.(2017a).Effect of a low cost parabolic reflector on the charging efficiency of an evacuated tube collector/storage system with a PCM. Solar Energy, 144, 758–766. https://doi.org/10.1016/j.solener.2017.01.073

[139] Sadeghi, G., Safarzadeh, H., & Ameri, M.(2018).Experimental and numerical investigations on performance of evacuated tube solar collectors with parabolic concentrator, applying synthesized Cu2O/distilled water nanofluid. Energy Sustainable Development/Energy for Sustainable Development, 48, 88–106. https://doi.org/10.1016/j.esd.2018.10.008

[140] Essa, M. A., Rofaiel, I. Y., & Ahmed, M. A.(2020).Experimental and Theoretical Analysis for the Performance of Evacuated Tube Collector Integrated with Helical Finned Heat Pipes using PCM Energy Storage. Energy, 206, 118166. https://doi.org/10.1016/j.energy.2020.118166

[141] Agade, P. K.(2025).Experimental Study of an Optimized Evacuated Tube Collector with Wavy Tape and Phase Change Material for Hot Water Production. Research Square(Research Square).https://doi.org/10.21203/rs.3.rs-6252758/v1

[142] Senobar, H., Aramesh, M., & Shabani, B.(2021).Evacuated tube solar thermal collector with enhanced phase change material thermal storage: An experimental study. Journal of Energy Storage, 46, 103838. https://doi.org/10.1016/j.est.2021.103838

[143] Deshmukh, K. B., Karmare, S., Sargar, T., Benschwartz, R., Varkute, N., Vengadesan, E., & Nehe, S.(2025).Heat transfer, friction factor, and performance evaluation of U-pipe evacuated tube solar thermal collector with TiN nanofluid and twisted tape inserts. Journal of Renewable Energy and Environment, 12(2),40-59

[144] Sobhansarbandi, S., Martinez, P. M., Papadimitratos, A., Zakhidov, A., & Hassanipour, F.(2017).Evacuated tube solar collector with multifunctional absorber layers. Solar Energy, 146, 342–350. https://doi.org/10.1016/j.solener.2017.02.038

[145] Manirathnam, A., Manikandan, M. D., Prakash, R. H., Kumar, B. K., & Amarnath, M. D.(2020).Experimental analysis on solar water heater integrated with Nano composite phase change material(SCi and CuO).Materials Today Proceedings, 37, 232–240. https://doi.org/10.1016/j.matpr.2020.05.093

[146] Kumar, P. M., & Mylsamy, K.(2020).A comprehensive study on thermal storage characteristics of nano-CeO2 embedded phase change material and its influence on the performance of evacuated tube solar water heater. Renewable Energy, 162, 662–676. https://doi.org/10.1016/j.renene.2020.08.122

[147] Yang, X., Lin, Q., Singh, P., Riaz, F., Agrawal, M. K., Alsenani, T. R., Xia, G. L., & Abdelmohimen, M. A.(2023).Evaluating the proficiency of a novel solar evacuated tube collector. Applied Thermal Engineering, 226, 120311. https://doi.org/10.1016/j.applthermaleng.2023.120311

[148] Elbrashy, A., Aboutaleb, F., El-Fakharany, M., & Essa, F. A.(2022).Experimental study of solar air heater performance with evacuated tubes connected in series and involving nano-copper oxide/paraffin wax as thermal storage enhancer. Environmental Science and Pollution Research, 30(2),4603–4616. https://doi.org/10.1007/s11356-022-22462-6

[149] Tabarhoseini, S. M., & Sheikholeslami, M.(2022).Modeling of evacuated tube solar collector involving longitudinal fins and nanofluids. Sustainable Energy Technologies and Assessments, 53, 102587. https://doi.org/10.1016/j.seta.2022.102587

[150] Ghaderian, J., Sidik, N. a. C., Kasaeian, A., Ghaderian, S., Okhovat, A., Pakzadeh, A., Samion, S., & Yahya, W. J.(2017).Performance of copper oxide/distilled water nanofluid in evacuated tube solar collector(ETSC)water heater with internal coil under thermosyphon system circulations. Applied Thermal Engineering, 121, 520–536. https://doi.org/10.1016/j.applthermaleng.2017.04.117

[151] Kumar, P. M., & Mylsamy, K.(2018).Experimental investigation of solar water heater integrated with a nanocomposite phase change material. Journal of Thermal Analysis and Calorimetry, 136(1),121–132. https://doi.org/10.1007/s10973-018-7937-9

[152] Abokersh, M. H., El-Morsi, M., Sharaf, O., & Abdelrahman, W.(2017a).On-demand operation of a compact solar water heater based on U-pipe evacuated tube solar collector combined with phase change material. Solar Energy, 155, 1130–1147. https://doi.org/10.1016/j.solener.2017.07.008

[153] Olfian, H., Ajarostaghi, S. S. M., Farhadi, M., & Ramiar, A.(2020).Melting and solidification processes of phase change material in evacuated tube solar collector with U-shaped spirally corrugated tube. Applied Thermal Engineering, 182, 116149. https://doi.org/10.1016/j.applthermaleng.2020.116149

[154] Kabeel, A., Abdelgaied, M., & Elrefay, M. K.(2020).Thermal performance improvement of the modified evacuated U-tube solar collector using hybrid storage materials and low-cost concentrators. Journal of Energy Storage, 29, 101394. https://doi.org/10.1016/j.est.2020.101394

[155] Naghavi, Ong, K., Badruddin, I., Mehrali, M., Silakhori, M., & Metselaar, H.(2015).Theoretical model of an evacuated tube heat pipe solar collector integrated with phase change material. Energy, 91, 911–924. https://doi.org/10.1016/j.energy.2015.08.100

[156] Sheikholeslami, M., Farshad, S. A., Gerdroodbary, M. B., & Alavi, A. H. (2022). Impact of new multiple twisted tapes on treatment of solar heat exchanger. The European Physical Journal Plus, 137(1).https://doi.org/10.1140/epjp/s13360-021-02157-6

[157] Sheikholeslami, M., Jafaryar, M., Gerdroodbary, M. B., & Alavi, A. H. (2022). Influence of novel turbulator on efficiency of solar collector system. Environmental Technology & Innovation, 26, 102383. https://doi.org/10.1016/j.eti.2022.102383